Dynamic Price Jumps: the Performance of High Frequency Tests and Measures, and the Robustness of Inference*

Worapree Maneesoonthorn†, Gael M. Martin‡, Catherine S. Forbes§

August 15, 2018

Abstract

This paper provides an extensive evaluation of high frequency jump tests and measures, in the context of using such tests and measures in the estimation of dynamic models for asset price jumps. Specifically, we investigate: i) the power of alternative tests to detect individual price jumps, most notably in the presence of volatility jumps; ii) the frequency with which sequences of dynamic jumps are correctly identified; iii) the accuracy with which the magnitude and sign of a sequence of jumps, including small clusters of consecutive jumps, are estimated; and iv) the robustness of inference about dynamic jumps to test and measure design. Substantial differences are discerned in the performance of alternative methods in certain dimensions, with inference being sensitive to these differences in some cases. Accounting for measurement error when using measures constructed from high frequency data to conduct inference on dynamic jump models is also shown to have an impact. The sensitivity of inference to test and measurement construction is documented using both artificially generated data and empirical data on both the S&P500 stock index and the IBM stock price. The paper concludes by providing guidelines for empirical researchers who wish to exploit high frequency data when drawing conclusions regarding dynamic jump processes.

Keywords: *Price jump tests; Nonparametric jump measures; Hawkes process; Discretized jump diffusion model; Volatility jumps; Bayesian Markov chain Monte Carlo*

JEL Classifications: C12, C22, C58.

*This research has been supported by Australian Research Council Discovery Grants No. DP150101728 and DP170100729. We thank a co-editor and two anonymous referees for very helpful and constructive comments on an earlier draft of the paper. We are also grateful to John Maheu, Herman van Dijk, Maria Kalli and Jim Griffin, plus participants at the 11th Annual RCEA Bayesian Econometric Workshop (Melbourne, 2017), for very helpful comments on an earlier version of the paper.

†Melbourne Business School, The University of Melbourne, Australia.

‡Corresponding author. Department of Econometrics and Business Statistics, Monash University, Australia. Email: *gael.martin@monash.edu*.

§Department of Econometrics and Business Statistics, Monash University, Australia.

1 Introduction

Extreme movements (or 'jumps') in asset prices play an important role in the tail behaviour of return distributions, with the perceived risk (and, hence, risk premium) associated with this extreme behaviour differing from that associated with small and regular movements (see, Bates, 1996, and Duffie *et al.*, 2000, for early illustrations of this point, and Todorov and Tauchen, 2011, Maneesoonthorn *et al.*, 2012, and Bandi and Renò, 2016, for more recent expositions). Indeed, the modelling of jumps, in both the price itself and its volatility, has been given particular attention in the option pricing literature, where the additional risk factor implied by random jumps has helped explain certain stylized patterns in option-implied volatility (Merton, 1976; Bates, 2000; Duffie *et al.*, Eraker, 2004; Todorov, 2010; Maneesoonthorn *et al.*; Bandi and Renò). Evidence of price jump clustering in spot returns - whereby price and/or volatility jumps occur in consecutive time periods - has also been uncovered, with various approaches having been adopted to model this dynamic behaviour, including the common occurrence of price and volatility jumps over time (Chan and Maheu, 2002; Eraker *et al.*, 2003; Maheu and McCurdy, 2004; Fulop *et al.*, 2014; Aït-Sahalia *et al.*, 2015; Bandi and Renò; Maneesoonthorn *et al.*, 2017).

Coincident with the trend towards more sophisticated models for asset prices, the use of high-frequency intraday data to construct nonparametric measures of asset price variation - including the jump component thereof - has become wide-spread. Multiple alternative methods are now available to practitioners, both for testing for jumps and for measuring price variation in the presence of jumps, with some empirical analyses exploiting such measures in addition to, or as a replacement of, measurements based on end-of-day prices. In some cases, nonparametric measures are used to *directly* represent the relevant latent feature (Andersen *et al.*, 2003; Koopman *et al.*, 2005; Andersen *et al.*, 2007; Bollerslev *et al.* 2009; Corsi, 2009; Martin *et al.*, 2009; Busch *et al.*, 2011; Hansen *et al.*, 2012; Christensen *et al.,* 2014), whilst in other instances, a state space framework - with its attendant measurement errors - is used to absorb the inaccuracy of the measures induced by the use of a finite number of intraday returns in their construction (Barndorff-Nielsen and Shephard, 2002; Creal, 2008; Takahashi *et al.*, 2009; Dobrev and Szerszen, 2010; Maneesoonthorn *et al.*, 2012; Koopman and Scharth, 2013; Maneesoonthorn *et al.*, 2017).

Whilst this wealth of new measures reaps benefits by allowing more complex processes to be identified and estimated, it also presents challenges. Specifically, the variety of ways in which high frequency observations can be exploited, in particular in constructing jump test statistics and measuring jump variation, has the potential to yield conflicting inferential conclusions. Moreover, with respect to any particular method, failure to detect a true jump (or sequence of jumps), spurious detection of a non-existent jump (or jump sequence), and error in the measurement of jump magnitude and/or sign, may distort inference on the process assumed to be driving jumps, including its dynamics.

This paper provides an extensive investigation - in the context of dynamic jump models - of

the relative accuracy of the many high frequency jump tests and measures that are on offer, plus an assessment of the robustness of inference to the use of different methods. The work represents a substantial advance on the earlier work of Dumitru and Urga (2012), in which the focus is almost entirely on *testing* for jumps, and in the context of models in which the intensity of jumps was time-invariant. Our work explores the performance of such tests in the context of *dynamic* price jumps, and in the (possible) presence of jumps in volatility. We document the frequency with which price jumps - including sequences of such jumps - are correctly *identified* by each test, in the context of a variety of different models that are nested within two specifications for the jump intensity: one based on a Hawkes process (Fulop *et al.*, 2014; Aït-Sahalia *et al.*, 2015; Maneesoonthorn *et al.*, 2017) and another functionally dependent on the volatility (Bates, 1996; Pan, 2002; Eraker, 2004; Maneesoonthorn *et al.*). Stochastic volatility - with the potential for dynamic jumps therein - is also accommodated within the experimental design. Two aspects of price jump *measurement* are next investigated: first, the accuracy with which the average *magnitude* of a sequence of jumps - including small clusters of consecutive jumps - is estimated, and second, the extent to which the correct jump *sign* is pinpointed across a sequence of time periods. We then investigate the *robustness* of Bayesian posterior inference for a discretized jump diffusion model to the use of different measures (and associated preliminary tests) using both artificial and empirical data. In order to highlight the impact of the characteristics of the data on the sensitivity, or otherwise, of posterior inference to measurement choice, data from 2005 to 2018 on both the S&P500 index and the IBM stock price is used in the empirical exercise. The influence of important tuning parameters used in the preliminary tests is also documented, with the paper concluding with a set of guidelines for practitioners on price jump test and measurement choice.

We begin, in Section 2, by providing a comprehensive review of ten alternative price jump tests that have been proposed. We group these ten methods into four categories: i) those based on the difference between a measure of total (squared) variation and a jump-robust measure of integrated variation (Barndorff-Nielsen and Shephard, 2004, 2006; Huang and Tauchen, 2005; Corsi *et al.*, 2010; Andersen *et al.*, 2012); ii) those that exploit measures of higher-order variation (Aït-Sahalia and Jacod, 2009; Podolskij and Ziggel, 2010); iii) those based on returns, rather than measures of variation (Andersen *et al.*, 2007; Lee and Mykland, 2008); and iv) those that exploit variance swaps (Jiang and Oomen, 2008). An outline of how each test can be used to extract various price jump measures is then given in Section 3. Using a simulation design that mimics a realistic empirical setting, the size and power performance of the various tests is assessed in Section 4.1. In contrast to Dumitru and Urga (2012), who investigate the effect of sampling frequency on test performance, we document test performance only in the context of the five-minute sampling frequency that has become the default in the literature, with particular emphasis given to the (potential) distorting impact of concurrent jumps in volatility.[1] The ability of the different methods to identify and

[1] This focus on the conventional five-minute sampling interval also deviates from the approach adopted in Christensen *et al.* (2014), in which the link between increased sampling frequency (and the attendant microstructure noise) and the proportion of total variation identified as price jump variation is explored.

accurately measure a sequence of jumps, including clusters of consecutive jumps, is then documented in Section 4.2, with a discussion of the various tuning choices given in Section 4.3.

Based on our findings in Section 4, in Section 5 four particular approaches are used to conduct inference about the dynamic characteristics of jumps within the discretized jump diffusion model, using artificially generated data in which the true characteristics of the process are known. Whilst a reasonable degree of robustness to method is documented, the use of a measure that performs relatively poorly in identifying sequences of jumps is found to yield less precise inference on the parameters controlling the jump dynamics. A further result highlighted therein is that accommodation of measurement error in the measures of price jump occurrence, magnitude and sign aids in the acquisition of accurate inference. The empirical illustration is outlined in Section 6, with dynamic jumps in both price *and* volatility accommodated via Hawkes processes. The impact on inferential results of certain important tuning parameters is documented. Section 7 provides some concluding remarks, including some guidelines on test and measure choice when inference on dynamic jump processes is the goal. All figures and tables are included at the end of the paper, and additional numerical results are provided in an on-line Supplementary Appendix.

2 Review of price jump tests

Defining $p_t = \ln(P_t)$ as the natural log of the asset price, P_t at time $t > 0$, we begin by assuming the following jump diffusion process for p_t,

$$dp_t = \mu_t dt + \sqrt{V_t} dW_t^p + dJ_t^p, \tag{1}$$

where W_t^p is the Brownian motion, and $dJ_t^p = Z_t^p dN_t^p$, with Z_t^p denoting the random price jump size and dN_t^p the increment of a discrete count process, with $P(dN_t^p = 1) = \delta^p dt$ and $P(dN_t^p = 0) = (1 - \delta^p)\, dt$.[2]

The aim of a price jump test is to detect the presence of the discontinuous component, dJ_t^p, and to conclude whether or not dN_t^p is non-zero over a particular period. The availability of high-frequency data has enabled various measures of variation - incorporating both the continuous and discontinuous components of (1) - to be constructed over a specified interval of time, e.g. one day, with the statistical properties of such measures established using in-fill asymptotics. The resulting distributional results are then utilized in the construction of a price jump test, where the null hypothesis is usually that the asset price is continuous over the particular interval investigated.

This section provides a review of a range of tests based on the concepts of, respectively, squared variation (Section 2.1), higher-order power variation (Section 2.2), standardized daily returns (Section 2.3) and variance swaps (Section 2.4). Our discussion is not limited to the technical construction of the tests, but also extends to issues related to implementation, including the role of tuning

[2] Introduction of an experimental setting that accommodates a dynamic process for the jump intensity parameter, δ^p, first occurs in Section 4.2.

parameters. Further discussion of tuning parameters is provided in Section 4.3, and the empirical impact of changes in certain of their values is explored in Section 6.[3]

2.1 Squared variation

The early literature on price jump testing exploits various measures of the squared variation of the asset price process. In the context of a continuous-time price process, as defined in (1), the object of interest is the difference between total quadratic variation over a discrete time period (typically a trading day), $Q\mathcal{V}_{t-1,t} = \int_{t-1}^{t} V_s ds + \sum_{t-1<s\leq t}^{N_t^p} (Z_s^p)^2$, and variation from the continuous component alone, quantified by the integrated variance, $\mathcal{V}_{t-1,t} = \int_{t-1}^{t} V_s ds$. By definition, the difference between these two quantities defines the contribution to price variation of the discontinuous jumps, $\mathcal{J}_{t-1,t}^2 = \sum_{t-1<s\leq t}^{N_t^p} (Z_s^p)^2$, and price jump test statistics can thus be constructed from the difference between *measures* of $Q\mathcal{V}_{t-1,t}$ and $\mathcal{V}_{t-1,t}$. In the following subsections, we briefly outline the Barndorff-Nielsen and Shephard (2004, 2006) approach, also exploited by Huang and Tauchen (2005), followed by two alternative tests proposed by Andersen *et al.* (2012) and Corsi *et al.* (2010) respectively, all of which exploit the difference in the squared variation measures. These tests are all one-sided upper-tail tests by construction.

2.1.1 Barndorff-Nielsen and Shephard (2004, 2006) and Huang and Tauchen (2005)

The test of Barndorff-Nielsen and Shephard (2004, 2006), denoted hereafter as BNS, is based on the difference between realized variance, $RV_t = \sum_{i=1}^{M} r_{t_i}^2$, and the corresponding bipower variation, $BV_t = \frac{\pi}{2}\left(\frac{M}{M-1}\right)\sum_{i=2}^{M} |r_{t_i}|\,|r_{t_{i-1}}|$, where $r_{t_i} = p_{t_i} - p_{t_{i-1}}$ denotes the i^{th} of M equally-spaced returns observed during day t. As has become standard knowledge, under (1), $RV_t \xrightarrow{p} Q\mathcal{V}_{t-1,t}$ and $BV_t \xrightarrow{p} \mathcal{V}_{t-1,t}$, as $M \to \infty$ (Barndorff-Nielsen and Shephard, 2002; Andersen *et al.*, 2003; BNS). Thus, $RV_t - BV_t \xrightarrow{p} \mathcal{J}_{t-1,t}^2$ as $M \to \infty$, and the decision regarding the occurrence of a price jump on day t can be based on testing whether or not $RV_t - BV_t$ is significantly larger than zero.

The joint (in-fill) asymptotic distribution of the two measures of squared volatility, RV_t and BV_t, appropriately scaled, has been established by BNS to be bivariate normal. Specifically, under the assumption of no price jumps (plus various regularity conditions),

$$\sqrt{\frac{M}{\mathcal{IQ}_{t-1,t}}}\begin{pmatrix} RV_t - \mathcal{V}_{t-1,t} \\ BV_t - \mathcal{V}_{t-1,t} \end{pmatrix} \xrightarrow{D} N\left(\begin{bmatrix} 0 \\ 0 \end{bmatrix}, \begin{bmatrix} 2 & 2 \\ 2 & \left(\frac{\pi}{2}\right)^2 + \pi - 3 \end{bmatrix}\right) \text{ as } M \to \infty. \tag{2}$$

The theoretical quantity $\mathcal{IQ}_{t-1,t} = \int_{t-1}^{t} V_s^2 ds$ is referred to as the integrated quarticity, an estimate of which can also be constructed from high-frequency returns data. For the purpose of the numerical investigations conducted in this paper, the following tripower quarticity measure is employed, $TP_t =$

[3] We note that there is some overlap between this outline of tests and that provided by Dumitru and Urga (2012). However, we feel it is important to establish our notation from the outset, as this enables us to highlight certain aspects of the tests (including tuning parameters) that are critical for the particular investigations that we pursue here. It also enables us to make precise the resulting jump measures that we exploit.

$\mu_{4/3}^{-3}\left(\frac{M^2}{M-2}\right)\sum_{i=3}^{M} \mid r_{t_{i-2}} \mid^{4/3} \mid r_{t_{i-1}} \mid^{4/3} \mid r_{t_i} \mid^{4/3}$, where $\mu_{4/3} = 2^{2/3}\Gamma(7/6)\Gamma(1/2)^{-1}$ and $TP_t \xrightarrow{p} \mathcal{IQ}_{t-1,t}$ as $M \to \infty$.

The limiting distribution in (2) allows for the construction of a variety of hypothesis tests for price jumps (Huang and Tauchen, 2005). Arguably, the most frequently-used of such tests is based on the relative price jump measure, $RJ_t = (RV_t - BV_t)/RV_t$, with the corresponding price jump test statistic,

$$T_{BNS,t} = \frac{RJ_t}{\sqrt{\left(\left(\frac{\pi}{2}\right)^2 + \pi - 5\right) M^{-1} \max\left(1, \frac{TP_t}{BV_t^2}\right)}}, \tag{3}$$

being standard normal under the null hypothesis of no jumps as $M \to \infty$. Consistent with the subscript in (3), we refer to this test as the BNS test.

2.1.2 Corsi, Pirino and Renò (2010)

Corsi, Pirino and Renò (2010), hereafter CPR, propose a test that is also based on the discrepancy between realized variance and a jump-robust estimator of the integrated variance. However, instead of employing the BV_t measure for the latter, and the TP_t measure of $\mathcal{IQ}_{t-1,t}$, they use the threshold measures, $CTBV_t = \frac{\pi}{2}\left(\frac{M}{M-1}\right)\sum_{i=2}^{M} \tau_1\left(r_{t_i}, \vartheta_{t_i}\right)\tau_1\left(r_{t_{i-1}}, \vartheta_{t_{i-1}}\right)$ and $CTriPV_t = \mu_{4/3}^{-3}\left(\frac{M^2}{M-2}\right)\sum_{i=3}^{M} \tau_{4/3}\left(r_{t_i}, \vartheta_{t_i}\right)\tau_{4/3}\left(r_{t_{i-1}}, \vartheta_{t_{i-1}}\right)\tau_{4/3}\left(r_{t_{i-2}}, \vartheta_{t_{i-2}}\right)$, respectively, where $\mu_{4/3}^{-3}$ is as defined in the previous section. The term $\tau_\zeta\left(r_{t_i}, \vartheta_{t_i}\right)$ denotes the so-called 'truncating function' for the absolute return raised to the power ζ, and ϑ_{t_i} denotes the threshold level such that any returns that satisfy $r_{t_i}^2 > \vartheta_{t_i}$ are truncated at $\vartheta_{t_i} = c_\vartheta^2 \widehat{V}_{t_i}$, where $\widehat{V}_{t_i}$ denotes a local variance estimator, reflecting the level of spot volatility at time t_i, and c_ϑ is a constant. For the value of $c_\vartheta = 3$ that is recommended, the relevant truncating functions proposed by CPR then take the form,

$$\tau_1\left(r_{t_i}, \vartheta_{t_i}\right) = \begin{cases} |r_{t_i}| & r_{t_i}^2 < \vartheta_{t_i} \\ 1.094\sqrt{\vartheta_{t_i}} & r_{t_i}^2 > \vartheta_{t_i} \end{cases}$$

and

$$\tau_{4/3}\left(r_{t_i}, \vartheta_{t_i}\right) = \begin{cases} |r_{t_i}|^{4/3} & r_{t_i}^2 < \vartheta_{t_i} \\ 1.129\vartheta_{t_i}^{2/3} & r_{t_i}^2 > \vartheta_{t_i} \end{cases}.$$

The resultant test statistic is defined as

$$T_{CPR,t} = \frac{1 - \frac{CTBV_t}{RV_t}}{\sqrt{\left(\left(\frac{\pi}{2}\right)^2 + \pi - 5\right) M^{-1} \max\left(1, \frac{CTriPV_t}{CTBV_t^2}\right)}}, \tag{4}$$

which, under the null hypothesis of no jumps, is also standard normal as $M \to \infty$.[4] We refer to the test based on the statistic in (4) as the CPR test.

[4]Note that, in contrast to the formulation of the CPR procedure summarized in Dumitru and Urga (2012), the truncating functions proposed by CPR are seen to differ depending on the power, ζ, to which the absolute return is raised.

2.1.3 Andersen, Dobrev and Schaumburg (2012)

Andersen, Dobrev and Schaumburg (2012), hereafter referred to as ADS, propose alternative measures of $\mathcal{V}_{t-1,t}$ based on the squared variation of the minimum and the median of adjacent absolute returns,

$$MinRV_t = \frac{\pi}{\pi - 2}\left(\frac{M}{M-1}\right)\sum_{i=2}^{M}\min\left(\left|r_{t_i}\right|,\left|r_{t_{i-1}}\right|\right)^2 \text{ and}$$

$$MedRV_t = \frac{\pi}{\pi + 6 - 4\sqrt{3}}\left(\frac{M}{M-2}\right)\sum_{i=3}^{M} med\left(\left|r_{t_i}\right|,\left|r_{t_{i-1}}\right|,\left|r_{t_{i-2}}\right|\right)^2,$$

respectively, with *large* returns thereby eliminated from the calculation. Taking the minimum and median of adjacent absolute returns also effectively imposes adaptive truncation, with the threshold for the truncation determined by neighbouring returns. Such an adaptive truncation scheme is arguably advantageous over the (fixed) threshold approach of CPR, as it avoids the need to make a subjective choice of local variance estimator.

Both $MinRV_t$ and $MedRV_t$ are consistent estimators of $\mathcal{V}_{t-1,t}$, and the resulting asymptotic properties of these estimators can be exploited to construct price jump tests in a similar fashion to those advocated under the BNS and CPR frameworks, with

$$T_{MinRV,t} = \frac{1 - \frac{MinRV_t}{RV_t}}{\sqrt{1.81M^{-1}\max\left(1, \frac{MinRQ_t}{MinRV_t^2}\right)}} \tag{5}$$

and

$$T_{MedRV,t} = \frac{1 - \frac{MedRV_t}{RV_t}}{\sqrt{0.96M^{-1}\max\left(1, \frac{MedRQ_t}{MedRV_t^2}\right)}} \tag{6}$$

each converging to standard normal variables as $M \to \infty$ under the null hypothesis of no jumps. The terms $MinRQ_t$ and $MedRQ_t$ denote the corresponding minimum and median measures of $\mathcal{IQ}_{t-1,t}$, constructed, respectively, as $MinRQ_t = \frac{\pi}{3\pi-8}\left(\frac{M^2}{M-1}\right)\sum_{i=2}^{M}\min\left(\left|r_{t_i}\right|,\left|r_{t_{i-1}}\right|\right)^4$ and $MedRQ_t = \frac{3\pi}{9\pi+72-52\sqrt{3}}\left(\frac{M^2}{M-2}\right)\sum_{i=3}^{M} med\left(\left|r_{t_i}\right|,\left|r_{t_{i-1}}\right|,\left|r_{t_{i-2}}\right|\right)^4$. The tests based on the statistics in (5) and (6) are hereafter referred to as the MINRV and MEDRV tests, respectively.

2.2 Higher-order $\mathcal{P}$-power variation

A second class of price jump test exploits the behaviour of higher-order $\mathcal{P}$-power variation, and estimators thereof. Following Barndorff-Nielson and Shephard (2004), let an estimator of the $\mathcal{P}$-power variation of p_t be defined as $\widehat{B}\left(\mathcal{P}, \Delta_M\right)_t = \sum_{i=1}^{M}\left|r_{t_i}\right|^{\mathcal{P}}$, where $\Delta_M = 1/M$ denotes the common length of the time intervals between consecutive returns, and $\mathcal{P} > 0$. The limiting behaviour of this estimator, for different values of $\mathcal{P}$, sheds light on the different components of the variation in p_t. In the case of $\mathcal{P} = 2$, $\widehat{B}\left(\mathcal{P}, \Delta_M\right)_t \xrightarrow{p} Q\mathcal{V}_{t-1,t}$ as $M \to \infty$, as is consistent with the distributional

result that $RV_t \xrightarrow{p} Q\mathcal{V}_{t-1,t}$. For $0 < \mathcal{P} < 2$,

$$\frac{\Delta_M^{1-\mathcal{P}/2}}{m_{\mathcal{P}}} \widehat{B}\left(\mathcal{P}, \Delta_M\right)_t \xrightarrow{p} A\left(\mathcal{P}\right)_t \text{ as } M \to \infty, \tag{7}$$

where

$$A\left(\mathcal{P}\right)_t = \int_{t-1}^{t} \left|V_s^{1/2}\right|^{\mathcal{P}} ds, \tag{8}$$

denotes the $\mathcal{P}$-power *integrated* variation, $m_{\mathcal{P}} = E\left(\left|U\right|^{\mathcal{P}}\right) = \pi^{-1/2} 2^{\mathcal{P}/2} \Gamma\left(\frac{\mathcal{P}+1}{2}\right)$ and U denotes a standard normal random variable. In contrast, for $\mathcal{P} > 2$, the increments from the jump component dominate, and the estimator converges in probability to the $\mathcal{P}$-power *jump* variation, $B\left(\mathcal{P}\right)_t = \sum_{t-1<s\leq t} \left|dJ_s\right|^{\mathcal{P}}$. If the jump component in (1) is not present and p_t is continuous as a consequence, then the limiting result in (7) holds for any $\mathcal{P} > 0$.

These limiting results can be used in a variety of ways to detect jumps. For example, Aït-Sahalia and Jacod (2009) compare $\widehat{B}\left(\mathcal{P}, \Delta_M\right)_t$ constructed over two different sampling intervals, while Podolskij and Ziggel (2010) rely on the limiting distribution of a modified version of $\widehat{B}\left(\mathcal{P}, \Delta_M\right)_t$. These two approaches are outlined briefly in the subsequent sections.

2.2.1 Aït-Sahalia and Jacod (2009)

The test of Aït-Sahalia and Jacod (2009) (ASJ hereafter) exploits the fact that for any positive integer $k \geq 2$, and on the assumption that p_t is continuous, the ratio

$$\widehat{S}\left(\mathcal{P}, k, \Delta_M\right)_t = \frac{\widehat{B}\left(\mathcal{P}, k\Delta_M\right)_t}{\widehat{B}\left(\mathcal{P}, \Delta_M\right)_t}, \tag{9}$$

converges in probability to $k^{\mathcal{P}/2-1}$. Further, they define the standardized test statistic

$$T_{ASJ,t} = \left(\widehat{\Sigma}_{M,t}^{c}\right)^{-1/2} \left(\widehat{S}\left(\mathcal{P}, k, \Delta_M\right)_t - k^{\mathcal{P}/2-1}\right), \tag{10}$$

with $\widehat{\Sigma}_{M,t}^{c} = \Delta_M M\left(\mathcal{P}, k\right) \widehat{A}\left(2\mathcal{P}, \Delta_M\right)_t / \widehat{A}\left(\mathcal{P}, \Delta_M\right)_t^2$. The term $\widehat{A}\left(\mathcal{P}, \Delta_M\right)_t$ denotes the truncated $\mathcal{P}$-power integrated variation estimator,

$$\widehat{A}\left(\mathcal{P}, \Delta_M\right)_t = \frac{\Delta_M^{1-\mathcal{P}/2}}{m_{\mathcal{P}}} \sum_{i=1}^{M} \left|r_{t_i}\right|^{\mathcal{P}} \mathbf{1}_{\left\{\left|r_{t_i}\right| < \vartheta \Delta_M^{\varpi}\right\}}, \tag{11}$$

and $M\left(\mathcal{P}, k\right) = \frac{1}{m_{\mathcal{P}}^2}\left(k^{\mathcal{P}-2}\left(1+k\right) m_{2\mathcal{P}} + k^{\mathcal{P}-2}\left(k-1\right) m_{\mathcal{P}}^2 - 2k^{\mathcal{P}/2-1} m_{k,\mathcal{P}}\right)$, where $m_{\mathcal{P}}$ is defined following (8), $m_{k,\mathcal{P}} = E\left(\left|U\right|^{\mathcal{P}} \left|U + \sqrt{k-1}V\right|^{\mathcal{P}}\right)$, and where V is a standard normal variable independent of U. The indicator function $\mathbf{1}_{\left\{\left|r_{t_i}\right| < \vartheta\left(\Delta_M\right)^{\varpi}\right\}}$ equals one if the absolute return is smaller than the threshold value, $\vartheta \Delta_M^{\varpi}$, serving as a truncation trigger in the estimation of (8). ASJ show that when $\mathcal{P} > 2$, $\vartheta > 0$ and the root exponent, ϖ, is in the range $\varpi \in (1/2 - 1/\mathcal{P}, 1/2)$, then the test statistic in (10) is asymptotically standard normal as $M \to \infty$. The critical region for the test based on (10) (referred to as the ASJ test from hereon in) is defined in the lower tail of the limiting distribution, since the limit of the ratio $\widehat{S}\left(\mathcal{P}, k, \Delta_M\right)_t$ in (9) is one when a jump

is present[5] - a quantity that is always lower than $k^{\mathcal{P}/2-1}$. The ASJ test statistic requires five tuning components to be selected: the order of power variation, $\mathcal{P}$; the time interval length, Δ_M; the integer defining the multiples of the time interval, k; the truncation scale factor, ϑ; and the truncation root, ϖ. The authors suggest using $\mathcal{P} = 4$, which is a conservative choice aimed at striking a balance between the power of the test to detect jumps and the quality of approximation of the (null) sampling distribution. They also advise that k should be chosen such that it is 'not too big', with no significant differences in (their) simulation experiments detected for $k = 2, 3, 4$, and a value of $k = 2$ deemed to be reasonable. The choice of truncation level, $\vartheta\Delta_M^{\varpi}$, determines the point at which to discriminate between continuous movements and price jumps, and is key to the computation of (11). With the asymptotic theory restricting the range of the truncation root to $\varpi \in (1/2 - 1/\mathcal{P}, 1/2)$, ASJ suggest taking ϖ close to the upper bound, specifically 0.48. They further advise that the truncation scale factor, ϑ, should be between 3 to 5 times the average value of (an estimate of) the diffusive variance, $\left(\int_0^t V_s ds\right)^{1/2}$. All such recommended values of the tuning components are employed in all implementations of the AJS test herein, along with a truncation scheme that is 3 times the diffusive volatility estimate, $\sqrt{BV_t}$.

2.2.2 Podolskij and Ziggel (2010)

Poldolskij and Ziggel (2010) (PZ hereafter) propose a price jump test based on the standardized statistic

$$T_{PZ,t} = \frac{\hat{B}_T(\mathcal{P}, \Delta_M)}{\sqrt{Var(\eta_i)\,\hat{B}_T(2\mathcal{P}, \Delta_M)}}, \tag{12}$$

where

$$\hat{B}_T(\mathcal{P}, \Delta_M) = M^{\frac{\mathcal{P}-1}{2}} \sum_{i=1}^{M} |r_{t_i}|^{\mathcal{P}} \left(1 - \eta_i \mathbf{1}_{\left\{|r_{t_i}| < \vartheta(\Delta_M)^{\varpi}\right\}}\right). \tag{13}$$

PZ demonstrate that for $\mathcal{P} \geq 2$, $T_{PZ,t}$ is asymptotically standard normal as $M \to \infty$, under the null hypothesis of no price jumps. Note that the test statistic involves the generation of an auxiliary independent and identically distributed random variable, η_i, from a distribution that is symmetric around 1, with $E(\eta_i) = 1$, $Var(\eta_i) < \infty$ and $E\left(|\eta_i|^{2+d}\right) > 0$ for some $d > 0$. The authors recommend simulating η_i from the distribution $P^{\eta} = \frac{1}{2}(\varsigma_{1-\tau} + \varsigma_{1+\tau})$, where ς is the Dirac measure and τ is a small constant with a value of 0.1 or 0.05. They also suggest truncation values of $\vartheta = 2.3\sqrt{BV_t}$, and $\varpi = 0.4$, respectively, with the value of 2.3 defining the 99^{th} percentile of the standard normal distribution and, thus, serving as a basis for discriminating between continuous movements (Gaussian) and jumps (non-Gaussian). The power term ϖ is bounded between 0 and $\frac{1}{2}$, with larger values of ϖ ensuring a faster convergence of the threshold estimator in (13) to $A(\mathcal{P})_t$. However, PZ argue that if the value of ϖ is too large, there is a higher probability of large but

[5] ASJ also derive a test using the limiting distribution of $\widehat{S}(\mathcal{P}, k, \Delta_M)_t$ under the null hypothesis that p_t contains jumps. However, one of the key assumptions needed to derive this asymptotic result is that jumps in p_t may not occur simultaneously with any jumps in the diffusive variance process, V_t. As such an assumption is rather restrictive, and given the large number of tests that are already under consideration in this paper, we have chosen to focus solely on the test derived under the assumption of continuity.

still continuous increments being identified as jumps; hence PZ propose the use of a smaller value ($\varpi = 0.4$) than do ASJ ($\varpi = 0.48$). In this paper, we implement two versions of the test based on (12), under the two power settings, $\mathcal{P} = 2$ and $\mathcal{P} = 4$, denoted respectively by PZ2 and PZ4, and each with τ set at 0.05.

2.3 Standardized returns

An alternative framework to one in which price jump test statistics are constructed from various measures of variation, is one that considers the behaviour of (appropriately standardized) returns themselves. In brief, based on the assumption of Brownian motion for the asset price, the return computed over an arbitrarily chosen interval length and scaled by the square root of a consistent estimator of the corresponding integrated variance, should be asymptotically standard normal if price jumps are absent. Two tests that exploit this property are discussed in this section.

2.3.1 Andersen, Bollerslev and Dobrev (2007)

Andersen, Bollerslev and Dobrev (2007), ABD hereafter, propose a simple method for extracting information about price jumps, making use of both intraday returns and estimates of integrated variance. The key to detecting price jumps in this framework is to recognize that intraday returns, standardized by a consistent estimator of the integrated volatility, given by

$$T_{ABD,t_i} = \frac{r_{t_i}}{\sqrt{M^{-1}BV_t}}, \tag{14}$$

is approximately standard normal when jumps are absent and under the assumption that volatility is locally constant over the trading day. Price jumps can thus be detected using the characteristics of standard normal distributions, with a price jump deemed to be present if $|T_{ABD,t_i}| > \Phi^{-1}\left(1 - \frac{\alpha^*}{2}\right)$, where $\alpha^* = 1 - (1-\alpha)^{1/M}$ denotes the Bonferroni adjusted significance level, given the (daily) significance level α, and $\Phi^{-1}(\cdot)$ denotes the inverse of the standard normal cumulative distribution function. The use of the Bonferroni adjustment addresses the issue of multiple testing, as this test is conducted M times throughout the trading day. ABD suggest that a conservative choice should be used for α, and document that the test performs satisfactorily in terms of producing the nominal size, along with sufficient power, at the significance level of $\alpha = 1 \times 10^{-5}$ (or 0.001%). We refer to the test based on the statistic in (14) as the ABD test.

2.3.2 Lee and Mykland (2008)

The approach of Lee and Mykland (2008), LM hereafter, was derived independently from that of ABD, but is based on the same idea of diffusive returns being conditionally Gaussian. LM propose a test statistic based on the maximum of the standardized returns, and characterize the distribution of the test statistic using extreme value theory. They argue that the use of normal quantiles, even with a Bonferroni style of adjustment, is too permissive, resulting in over-rejection of the null.

The LM test statistic is defined as

$$T_{LM,t}=\frac{\left(\max\left(\widetilde{T}_{LM,t_i}\right)-C_M\right)}{S_M}, \tag{15}$$

where $\widetilde{T}_{LM,t_i}=\frac{|r_{t_i}|}{\sqrt{\hat{V}_{t_i}}}$, $C_M=\frac{(2\log M)^{1/2}}{0.8}-\frac{\log\pi+\log(\log M)}{1.6(2\log\pi)^{1/2}}$, $S_M=\frac{1}{0.6(2\log\pi)^{1/2}}$, $\hat{V}_{t_i}$ denotes the local variance estimate and $\max\left(\widetilde{T}_{LM,t_i}\right)$ is defined over the M intra-period returns. LM demonstrate that under the null of no jumps, the statistic in (15) converges to the standardized Gumbel distribution, G, as $M\to\infty$, with the null hypothesis of no jump rejected if the test statistic falls above the upper tail critical value. LM suggest that the point-in-time variance estimate be defined as $\hat{V}_{t_i}=\frac{BV_{t_i}}{K-2}$, where $BV_{t_i}=\frac{\pi}{2}\left(\frac{K}{K-1}\right)\sum_{j=i-K+2}^{i}|r_{t_j}||r_{t_{j-1}}|$ is the bipower variation estimated over the window size K up to and including time t_i. We use $K=10$ in the numerical work in the paper.

2.4 Variance swaps - Jiang and Oomen (2008)

Variance swaps are instruments made up of financial assets and/or derivatives and are used as tools to hedge against volatility risk. The payoff of a variance swap can be replicated by taking a short position in the so-called "log contract" and a long position in the underlying asset, with the long position being continuously re-balanced (see Neuberger, 1994). The payoff of such a replicating strategy, computed as the accumulated difference between proportional returns and continuously compounded logarithmic returns, equates to half of the integrated variance under the assumption of no price jump. When a jump is present, the replication error is completely determined by the realized jump.

Jiang and Oomen (2008), JO hereafter, exploit this concept by considering a function of the difference between the i^{th} arithmetic return, R_{t_i}, and the i^{th} log return, r_{t_i},

$$SwV_t=2\sum_{i=1}^{M}\left(R_{t_i}-r_{t_i}\right), \tag{16}$$

with associated probability limit,

$$p\lim\left(SwV_t-RV_t\right)=\begin{cases}0 & \text{when } p_t\in\Omega_t^c\\ 2\int_{t-1}^{t}\left(\exp\left(Z_s\right)-Z_s-1\right)dN_s^p-\int_{t-1}^{t}Z_s^2dN_s^p & \text{when } p_t\in\Omega_t^j\end{cases}. \tag{17}$$

The set Ω_t^j is that which contains all non-continuous (jump) price processes and Ω_t^c is the set containing all continuous price processes. JO propose a number of test statistics based on (16), but here we consider only

$$T_{JO,t}=\frac{BV_t}{M^{-1}\sqrt{\widehat{\Omega}_{SwV}}}\left(1-\frac{RV_t}{SwV_t}\right), \tag{18}$$

where $\widehat{\Omega}_{SwV}=3.05\frac{M^3}{M-3}\sum_{i=1}^{M}\prod_{k=0}^{3}\left|r_{t_{i-k}}\right|^{3/2}$ is a consistent estimator of $\int_{t-1}^{t}V_s^3ds$. Under the null of no jumps, $T_{JO,t}$ converges to a standard normal distribution as $M\to\infty$. Since SwV_t-RV_t tends to be positive when the price jump is positive and negative when price jump is negative, the JO test based on (18) is conducted as a two-sided test in which the *sign* of the jump is detected in addition to its presence.

3 Extracting measures of jump occurrence, size and sign

As already highlighted, one of the primary aims of this paper is to assess the impact of different high frequency jump measures on price jump inference. That is, in addition to the detection (or otherwise) of price jumps, the ten tests outlined in Section 2 enable alternative nonparametric *measures* of price jumps - both the occurrence and magnitude thereof - to be extracted. These nonparametric measures, in turn, contain information about the dynamics of price jumps which, when allied with a theoretical model, can be used to draw empirical conclusions about the dynamic behaviour of extreme price movements. It is the robustness (or otherwise) of inferential results to the choice of nonparametric measure that is to be explored later in the paper.

For all ten tests, the price jump *occurrence* indicator, $I^p_{*,t}$, is defined as

$$I^p_{*,t} = \mathbf{1}\left(T_{*,t} \in C_*\left(\alpha\right)\right), \tag{19}$$

where $C_*\left(\alpha\right)$ denotes the critical region of test '$*$' (given by the relevant abbreviation), defined by significance level α, and with associated statistic $T_{*,t}$. The indicator thus equals one when the relevant test concludes in favour of a jump, and equals zero otherwise.

The method of extracting the price jump *size*, $\widetilde{Z}^p_{*,t}$, depends however on the particular test being used. Tauchen and Zhou (2011), for example, use the BNS approach to define

$$\widetilde{Z}^p_{BNS,t} = sign\left(r_t\right) \times \sqrt{\max\left(RV_t - BV_t, 0\right)}, \tag{20}$$

with the assumption adopted that the *sign* of the price jump is equivalent to the sign of the daily return over the day. Indeed, for all tests that utilize squared and higher-order $\mathcal{P}$-power variation, this same approach to (signed) measurement can be adopted, with the appropriate measure of integrated variance simply replacing BV_t in (20). For example, the (signed) jump size for the CPR approach can be computed as

$$\widetilde{Z}^p_{CPR,t} = sign\left(r_t\right) \times \sqrt{\max\left(RV_t - CTBV_t, 0\right)},$$

while the $MedRV_t$ and $MinRV_t$ measures can replace BV_t under the ADS approach. Similarly, the truncated power variation for $\mathcal{P} = 2$ can be used to extract signed jump sizes associated with the ASJ and PZ (2 and 4) tests, in conjunction with the truncation schemes used in constructing the test statistics themselves.

Extracting $\widetilde{Z}^p_{*,t}$ within the ABD and LM frameworks requires a different approach. ABD suggest that the aggregated price jumps over a trading day be computed as

$$\widetilde{Z}^p_{ABD,t} = \sum_{i=1}^{M} r_{t_i} \mathbf{1}\left(\left|T_{ABD,t_i}\right| > \Phi^{-1}\left(1 - \frac{\alpha^*}{2}\right)\right).$$

The sign of $\widetilde{Z}^p_{ABD,t}$ then depends on the sign of the sum of the returns that contribute to the aggregation itself. LM have not entertained this, but since the principle that underlies the construction

of their test is identical to that of ABD, we note that a comparable approach (but with $\widetilde{T}_{LM,t_i}$ replacing T_{ABD,t_i}) is available.

The JO approach provides yet another avenue for extracting information about price jump size. Building on the relationship given in (17), with a daily discretization scheme, the price jump size $\widetilde{Z}^p_{JO,t}$, is one that satisfies

$$SwV_t - RV_t = 2\left(\exp\left(\widetilde{Z}^p_{JO,t}\right) - \widetilde{Z}^p_{JO,t} - 1\right) I^p_{JO,t} - \left(\widetilde{Z}^p_{JO,t}\right)^2 I^p_{JO,t}. \tag{21}$$

Thus, when a jump is detected under this approach, $\widetilde{Z}^p_{JO,t}$ is obtained as a solution to the above nonlinear relation. Note, with this approach, $\widetilde{Z}^p_{JO,t}$ incorporates the *sign* of the price jump in addition to its magnitude.

The time series of observed measures, $I^p_{*,t}$ and $\widetilde{Z}^p_{*,t}$, can be used to gain insight into the dynamics of price jumps and/or the impact of such dynamics on returns. For example, Andersen *et al.* (2010) use variants of the BNS-based measures ($I^p_{BNS,t}$ and $\widetilde{Z}^p_{BNS,t}$) to produce appropriate standardization of daily returns on the Dow Jones Industrial Average stocks. Tauchen and Zhou (2011) also use the BNS-based measures, but to evaluate the price jump dynamics of the S&P500, the 10-year US Treasury bond, and the US dollar/Japanese Yen exchange rate. Finally, Maneesoonthorn *et al.* (2017) use these same jump measures to supplement daily return and nonparametric volatility measures in a multivariate state space model for the S&P500 market index, treating these measures as being observed with error.

To date however, we are not aware of any study that provides a comprehensive assessment of *both* the full range of preliminary jump tests (as outlined in Section 2), *and* the associated set of measurements of jump occurrence, size and sign, including the accuracy with which these measurements pinpoint, respectively, the presence and magnitude of a sequence of dependent price jumps. We are also not aware of any study in which the impact on inference regarding price and/or volatility jump dynamics of using *different* measures is documented. It is these tasks that we now undertake in the remainder of the paper.

4 Assessment of test and measurement accuracy

We assess the performance of each jump detection and measurement method in artificial data scenarios. In Section 4.1 we document the power of each method to detect individual price jumps. As noted earlier, in contrast to the earlier assessment of test performance by Dumitru and Urga (2012), our simulation exercise is used to shed particular light on the robustness of the alternative price jump tests in the presence of a discontinuous volatility process. This is something that has not, to our knowledge, been documented elsewhere, for any of the tests discussed, and which is relevant to our empirical investigation, in which both (dynamic) price and volatility jumps are modelled. In Section 4.2 we then document the frequency with which a *sequence* of price jumps is correctly detected and measured, under two alternative dynamic specifications for the jump intensity. The accuracy of detection is assessed in Section 4.2.1, and Section 4.2.2 documents two aspects of price

jump measurement, namely: i) the accuracy of price jump *magnitude* measurement; and ii) the extent to which the correct *sign* of any price jump is found. Included in this is an assessment of the accuracy with which small clusters of consecutive jumps are measured. All numerical results regarding sequential jump detection and measurement are documented and discussed in Section 4.2.3. Section 4 ends with a brief discussion of the key tuning parameters that underpin test and measurement design, robustness to which is assessed in Section 6.

4.1 Detection of individual jumps: empirical size and power

In this section, we assess the ability of the ten jump tests (BNS, CPR, MINRV, MEDRV, ASJ, PZ2, PZ4, ABD, LM and JO) to correctly detect price jumps. Given the increased focus on allowing for volatility jumps in the empirical literature - including in our own empirical work in Section 6 - we document the power of such tests as the magnitude of a concurrent volatility jump increases.

With reference to (1), reproduced and re-numbered here for convenience,

$$dp_t = \mu_t dt + \sqrt{V_t} dW_t^p + dJ_t^p, \tag{22}$$

we now specify

$$\mu_t = \mu + \gamma V_t, \tag{23}$$

and define a jump diffusion process for V_t,

$$dV_t = \kappa \left(V_t - \theta \right) + \sigma_v \sqrt{V_t} dW_t^v + dJ_t^v, \tag{24}$$

where dW_t^v is assumed to be uncorrelated with dW_t^p, and $dJ_t^v = Z_t^v dN_t^v$, with Z_t^v denoting the random volatility jump size and dN_t^v the increment of a discrete count process, with $P(dN_t^v = 1) = \delta^v dt$ and $P(dN_t^v = 0) = (1 - \delta^v)\, dt$. For the purpose of this first simulation exercise, we set $\delta^p = \delta^v = 1$, which implies that both $dN_t^p = 1$ and $dN_t^v = 1$, for all t. Price and volatility jump sizes are then determined by a 100×100 grid of paired values given by $Z_t^p \in \left[-10\sqrt{\theta}, +10\sqrt{\theta} \right]$ and $Z_t^v \in [0, 20\theta]$. Non-zero values of Z_t^p and Z_t^v thus imply, with unit probability, that a jump in the price and volatility process, respectively, has in fact occurred, whilst zero values for Z_t^p and Z_t^v imply otherwise. The data is generated using true parameter values: $\mu = 0.2$, $\gamma = -7.9$, $\kappa = 0.03$, $\theta = 0.02$ and $\sigma_v = 0.02$ (adhering to the theoretical restriction $2\kappa\theta \geqslant \sigma_v^2$), and with the diffusive variance process initialized at θ.

For each scenario, a very fine Euler discretization is employed to simulate high-frequency observations, with 720 observations created per trading day, equivalent to generating price observations every 30 seconds. The price jump test statistics are then constructed using every 10^{th} observation over the daily interval, equivalent to the five-minute sampling frequency that is used throughout the paper. We then compute, over 1000 independent Monte Carlo iterations, the proportion of times that a test detects a price jump. Note that this proportion equates to the empirical size of the test when $Z_t^p = 0$ for all t, and the empirical *power* of the test otherwise. The nominal size of

each test is set at 1%. The results are summarized graphically in Figure 1, with the price jump magnitude (Z_t^p) on one axis, the simultaneous volatility jump magnitude (Z_t^v) on the other, and the proportion of times that the jump is detected using each method recorded on the vertical axis. Note that the results for PZ4 were very similar to those for PZ2 and have thus been omitted from the graphical display.

As can be observed from Panel E in Figure 1, the ASJ test has low power to detect sizeable price jumps, even when a volatility jump is absent ($Z_t^v = 0$). Once a volatility jump is also present, even one that is small in magnitude, the power of this test drops essentially to zero. The power curve of the ABD test in Panel G exhibits qualitatively similar behaviour, if much less extreme. Whilst the poor power properties of these two tests are in line with certain simulation results reported in Dumitru and Urga (2012), we are not aware of any study that has documented this severe impact of volatility jumps.

In contrast to the behaviour of the ASJ and ABD tests, the remaining seven tests display a much less extreme loss in power (for detecting price jumps) in the presence of volatility jumps. Of these, both the PZ2 and LM tests display a minimal change in the shape of their power curves (across the Z_t^p axis) as Z_t^v increases, although at the cost of quite severe size distortion (Panels F and H, respectively)[6]. That is, these two procedures incorrectly reject the true null of no price jump with higher and higher probability as the magnitude of the volatility jump increases. Noting that powers are computed as raw proportions, it is perhaps not surprising that these two procedures have the highest power of all nine shown, when variance jumps are present. As the size distortion changes with the magnitude of the volatility jump, full knowledge of this magnitude is required for any size correction to be performed. Given that this is not feasible in practical settings, we have chosen not to record size-adjusted powers. The remaining five tests, BNS, CPR, MINRV, MEDRV and JO (Panels A, B, C, D and I, respectively), all display relatively robust size properties in the presence of volatility jumps; however they all exhibit, to varying degrees, power curves that flatten near the origin (over the Z_t^p axis) as the magnitude of the volatility jump increases.

Finally, prompted by a referee, we also assess the power of these tests in the presence of microstructure noise, under both independent and identically distributed (*i.i.d.*) and autocorrelated noise assumptions. We find that, despite there being a slight drop in the level of the power curve for each test, the overall pattern of each curve remains as presented in Figure 1. This result is not surprising given that our experiments are conducted using the five-minute interval, a frequency that has been found to mitigate the effect of microstructure noise on realized measures (see Bandi and Russell, 2008, for an exploration of the optimal sampling frequency in the presence of microstructure noise). These additional results are documented in the on-line Supplementary Appendix.[7]

[6] We also investigated the performance of the LM test conducted with the form of simulated critical value proposed by Dimitru and Urga (2012) (as opposed to the asymptotic critical value from the Gumbel distribution). Results are in line with those documented in their paper, and the pattern in the power curves remains broadly consistent with that documented in Figure 1, Panel H, although the size distortion is even more pronounced. These additional results are provided in the Supplementary Appendix available on-line.

[7] As highlighted in Christensen *et al.* (2014), this mitigation of the impact of microstructure noise via the choice

4.2 Detection and measurement of a sequence of jumps

We now generate artificial data over a period of $T = 2000$ sequential 'days' using the model in (22)-(24) augmented by the following specifications. First, price and volatility jump occurrences now each arise from *dynamic* Poisson processes, given by $\Pr\left(dN_t^p = 1\right) = \delta_t^p dt$ and $\Pr\left(dN_t^v = 1\right) = \delta_t^v dt$, respectively. Only a single price and volatility jump is allowed to occur on each day, with δ_t^p and δ_t^v determining the probability of each of those jumps occurring. Two alternative specifications for δ_t^p are entertained, given by

$$\text{Hawkes (H): } d\delta_t^p = \alpha_p\left(\delta_\infty^p - \delta_t^p\right)dt + \beta_p dN_t^p \tag{25}$$

$$\text{State Dependent (SD): } \delta_t^p = \beta_{p0} + \beta_{p1} V_t. \tag{26}$$

The parameter δ_∞^p appearing in (25) is the steady state level of δ_t^p to which the price jump intensity reverts once the impact of 'self-excitation' (via dN_t^p) dissipates; see Hawkes (1971a,b). The unconditional mean intensity implied by the Hawkes process is

$$\delta_0^p = \frac{\alpha_p \delta_\infty^p}{\alpha_p - \beta_p}, \tag{27}$$

while that of the state dependent intensity is $\delta_0^p = \beta_{p0} + \beta_{p1} E\left(V_t\right)$.

One or other of the specifications in (25) and (26) have been used elsewhere to model dynamic price (and volatility) jump intensity (see, for example, Bates, 1996, Pan, 2002, Eraker, 2004, Aït-Sahalia *et al.*, 2015, and Maneesoonthorn *et al.*, 2017), and the two are employed here in order to examine the robustness (or otherwise) of the jump detection methods to different assumptions adopted for δ_t^p. In particular, the state dependent specification in (26) induces a smoother intensity process, following the pattern of the latent volatility process quite closely, while the Hawkes model in (25) typically produces sharp spikes following each jump event. Plots of representative examples of each process are presented in Figure 2 and discussed in Section 4.2.3, with the link between the distinctive features of each process and the accuracy with which sequences of jumps generated from each process are detected, also documented therein.

Associated with each of the two specifications for δ_t^p, we consider three different scenarios for volatility jumps: 1) volatility jumps are absent ($\delta_t^v = 0$ for all t) (corresponding to models labelled hereafter as SD1 and H1, respectively); 2) volatility jumps have a constant intensity ($\delta_t^v = \delta_0^v$) (Models SD2 and H2); and 3) the volatility jump intensity takes the same form as the price jump intensity ($\delta_t^v = \delta_t^p$), but with volatility and price jumps occurring independently one of the other (i.e. with dN_t^p and dN_t^v assumed to be independent random variables) (Models SD3 and H3). The

of the five-minute interval may come at a cost. Specifically, movements in the continuous component of the asset price that derive from a burst of (or jump in) volatility, and which may be correctly identified as such at a finer frequency (by tests suitably *adjusted* for microstructure noise), could be incorrectly diagnosed as a price jump at the five-minute interval. Given the prevalent use of five-minute data however, plus the use of tests that are *not* modified to cater for the presence of microstructure noise, we believe that our conclusions are particularly relevant to the typical practitioner. To adapt our investigations to cater for differing sampling frequencies - and tests/measures modified for microstructure noise - would be an interesting exercise, but certainly beyond the scope of the present paper.

parameters in (25) and (26) are chosen to ensure that the unconditional price jump intensity, δ_0^p, is the same for both models, with the parameter settings for all six scenarios described here recorded in Panel A of Table 1. Note that the parameter values are chosen to be broadly in line with those estimated using S&P500 data in both the empirical analysis in Maneesoonthorn *et al.* (2017) and the empirical illustration in Section 6.

In contrast to the settings adopted in Section 4.1 for price and volatility jump size (Z_t^p and Z_t^v, respectively) we now model these two latent variables explicitly as follows. The price jump size is specified as

$$Z_t^p = S_t^p \exp\left(M_t^p\right), \tag{28}$$

with the sign of the jump defined as

$$S_t^p = \begin{cases} -1 & \text{with probability } \pi_p \\ 1 & \text{with probability } 1-\pi_p \end{cases}, \tag{29}$$

and the logarithmic magnitude as

$$M_t^p \sim N(\mu_p, \sigma_p^2). \tag{30}$$

The (positive) volatility jump size is modelled as

$$Z_t^v \sim Exp\left(\mu_v\right), \tag{31}$$

where $\mu_v = 1.5 \times \theta$, with θ as appearing in (24). The parameter values used in specifying (28) to (31) are given in Panel B of Table 1, again with reference to empirical estimates recorded in Maneesoonthorn *et al.* (2017) and Section 6.

Using the simulated five-minute intraday data for each day, a sequence of $T = 2000$ price jump tests are conducted and the associated sequences of price jump occurrence ($I_{*,t}^p$) and size ($\widetilde{Z}_{*,t}^p$) computed for each test '$*$'. The intraday data are simulated as in Section 4.1, with occurrences of both price and volatility jumps restricted to one per day, as noted above. The accuracy measures associated with all methods are computed as averages over the $N = 1000$ Monte Carlo iterations of the simulated price sequence. Evaluation measures pertaining to the *detection* of the sequence price jumps are outlined in Section 4.2.1. Those related to the measurement of *magnitude* and *sign* of a sequence of jumps, including smaller clusters of consecutive jumps, are given in Section 4.2.2. Discussion of all numerical accuracy results then follows in Section 4.2.3.

4.2.1 Accuracy of sequential jump detection

For the purpose of documenting the accuracy of the price jump indicator measure, $I_{*,t}^p$ defined in (19), we estimate the probability of correctly detecting a price jump, $DJ^* = \Pr\left(I_{*,t}^p = 1 | \Delta N_t^p = 1\right)$, over the sequence of $T = 2000$ days. Specifically, for Monte Carlo iteration i, this conditional probability is estimated by $DJ_i^* = \sum_{t=1}^T \mathbf{1}\left(I_{*,t}^p = 1 \text{ and } \Delta N_t^p = 1\right) / \sum_{t=1}^T \Delta N_t^p$, with the average over the N Monte Carlo iterations then recorded, as

$$\overline{DJ^*} = \frac{1}{N} \sum\nolimits_{i=1}^N DJ_i^*.$$

We next perform the comparable calculation, estimating the probability of *not* detecting a jump, conditional on the actual absence of a jump, $NDJ^* = \Pr\left(I^p_{*,t} = 0 | \Delta N^p_t = 0\right)$, with

$$\overline{NDJ^*} = \frac{1}{N}\sum\nolimits_{i=1}^{N} NDJ^*_i$$

recorded, where $NDJ^*_i = \sum_{t=1}^{T} \mathbf{1}\left(I^p_{*,t} = 0 \text{ and } \Delta N^p_t = 0\right) / \sum_{t=1}^{T} \mathbf{1}(\Delta N^p_t = 0)$.

Frameworks in which $\overline{DJ^*}$ and $\overline{NDJ^*}$ are close to one are deemed to produce accurate price jump occurrence measurement. Ideally, however, the error sequence should also be independent over time so that an error at one time point does not alter the rate of error in subsequent periods. To this end we define the sequence of errors,

$$Err_{*,t} = \mathbf{1}\left(I^p_{*,t} \neq \Delta N^p_t\right),$$

for each method and, in the spirit of Christoffersen (1998), conduct a test of the null hypothesis that $Err_{*,t}$ is a sequence of independent Bernoulli draws for each Monte Carlo iteration of the sequence. We then record (over the Monte Carlo replications) the proportion of times that the null hypothesis is rejected, using the abbreviation SDE^* to denote the proportion of rejections in favour of the alternative of serially dependent errors. The approach with SDE^* closest to zero is preferred.

4.2.2 Accuracy of sequential (and clustered) jump measurement

As noted from (28), the latent price jump size at time t comprises two components: magnitude ($\exp M^p_t$) and sign (S^p_t), and the accuracy with which each component is measured, across the sequence of $T = 2000$ days, is considered separately. For all but the JO approach, the measured jump sign coincides exactly with the sign of the returns (see relevant details in Section 3).

The accuracy with which the true price jump *magnitude* is estimated is measured by the mean squared error (MSE) computed from the distance between the absolute values of the measurement, $\left|\widetilde{Z}^p_{*,t}\right|$, and the simulated price jump size $|Z^p_t|$. Specifically, the MSE is defined as

$$MSE^* = \frac{\sum_{t=1}^{T}\left(\left|\widetilde{Z}^p_{*,t}\right| - |Z^p_t|\right)^2 \Delta N^p_t}{\sum_{t=1}^{T} \Delta N^p_t},$$

with the approach producing the smallest MSE^* preferred. On the suggestion of the referees, we also compute the MSE for jumps that occur in *clusters* of two or more, and three or more, *consecutive* jumps, with these statistics denoted by $MSE^*_{\geq 2}$ and $MSE^*_{\geq 3}$, respectively.

The accuracy with which the price jump *sign* is pinpointed is measured by an estimate of the probability that the correct sign is identified, conditional on the occurrence of a jump

$$SCD^* = \Pr\left(sign\left(\widetilde{Z}^p_{*,t}\right) = sign\left(Z^p_t\right) | \Delta N^p_t = 1\right),$$

with this estimate given by

$$\overline{SCD^*} = \frac{1}{N}\sum\nolimits_{i=1}^{N} SCD^*_i,$$

where $SCD_i^* = \frac{\sum_{t=1}^{T} \Delta N_t^p \mathbf{1}\left(sign\left(\widetilde{Z}_{*,t}^p\right) = sign\left(Z_t^p\right)\right)}{\sum_{t=1}^{T} \Delta N_t^p}$ provides the corresponding estimated probability from the i^{th} Monte Carlo replicated sample. Large values of $\overline{SCD^*}$ are desired.

4.2.3 Numerical accuracy results

Tables 2 and 3 record the seven accuracy measures ($\overline{DJ^*}$, $\overline{NDJ^*}$, SDE^*, MSE^*, $MSE^*_{\geq 2}$ and $MSE^*_{\geq 3}$ and $\overline{SCD^*}$) for all ten approaches, under the Hawkes (25) and the state dependent (26) specifications, respectively. The figures that represent the *largest* values of $\overline{DJ^*}$, $\overline{NDJ^*}$ and $\overline{SCD^*}$, and the *smallest* values of SDE^*, MSE^*, $MSE^*_{\geq 2}$ and $MSE^*_{\geq 3}$ under any particular data generating process, are highlighted in bold.

First, we note that when volatility jumps are introduced, in specifications H2, H3, SD2 and SD3, all approaches exhibit a decline in accuracy according to all seven measures. This is consistent with the findings discussed in Section 4.1 regarding the robustness of price jump detection, with all relevant power curves being impacted in some way by an increase in the volatility jump size. Further, we find that the introduction of dynamics in the volatility jumps via the Hawkes specification (i.e. H3 versus H2) does not produce too marked an affect on performance, but that the move from SD2 to SD3, under the state dependent framework, results in a more notable reduction in accuracy.

A comparison of the corresponding evaluation measures shown in Tables 2 and 3 highlights the way in which the nature of the dynamic structure of the price jump intensity (δ_t^p) affects the accuracy with which the different aspects of the jump process are measured. Under the Hawkes process in (25), and for all settings for δ_t^v, all ten frameworks estimate the magnitude and sign of the price jump more accurately (i.e. MSE^* is lower and $\overline{SCD^*}$ is higher) than they do under the state dependent process in (26). While not uniformly true for the clustering measures, $MSE^*_{\geq 2}$ and $MSE^*_{\geq 3}$, this statement remains broadly applicable. Correct detection of price jumps ($\overline{DJ^*}$) also tends to be higher under the Hawkes process, whilst the (correct) detection of non-jump days ($\overline{NDJ^*}$) is very similar across the two tables. However, the errors associated with detecting price jumps, as indicated by SDE^*, tend to be more serially correlated under the Hawkes process. To understand why the latter may be the case, we refer to the representative single path (using the parameter settings given in Table 1) of the two jump intensity processes in Figure 2. As can be observed, despite the unconditional intensity for both processes being identical, the simulated dynamic paths are quite distinct. Movements in the Hawkes intensity (Panel A) are far more erratic, with sharp rises in the intensity induced by an occurrence of a past jump. In contrast, movements in the state dependent intensity (Panel B) are much less severe, reflecting the characteristics of the Brownian motion that drives the stochastic volatility process on which δ_t^p depends. As a result, the Hawkes intensity generates a greater degree of jump clustering than does the state dependent model, which is more difficult to discern, and with a greater degree of autocorrelation being found in the detection errors as a consequence.

We now turn to a discussion of each of the seven accuracy measures in turn - $\overline{DJ^*}$, $\overline{NDJ^*}$, SDE^*, $MSE^*, MSE^*_{\geq 2}$, $MSE^*_{\geq 3}$ and $\overline{SCD^*}$ - and to which of the ten frameworks, if any, is the

most accurate according to a specific measure. Both tables suggest that the PZ2 approach is most accurate in terms of *detecting* price jumps, with its $\overline{DJ}^*$ measure being the highest (and notably so in some instances) in all but one case (H1), where the PZ2 approach is a close second behind the JO approach. The $\overline{NDJ^*}$ measure, indicating the ability of an approach to correctly identify the absence of a price jump, is close to one for *all* approaches and for all data generating processes. Hence, although the top ranking alternates between the ASJ and PZ4 methods, the magnitudes of this recorded measure across all instances are so close that it could be argued that all approaches are equally accurate in discerning the absence of jumps.

The SDE^* measure, for which low values are indicative of independence in the jump detection errors, is seen - as noted above - to be sensitive to the nature of the dynamic structure of the price jump itself. Whilst all approaches perform worse according to this measure under the Hawkes specification, the ABD and ASJ approaches perform particularly poorly. Of all ten approaches both PZ2 and PZ4 prove to be the most robust across the six different price jump specifications (H1 to SD3), in terms of retaining reasonably small (and similar) values for SDE^*.

With regard to the accuracy with which price jump *magnitude* is estimated, the ASJ approach produces the smallest value of MSE^* in the absence of volatility jumps (specifications H1 and SD1), while the MEDRV approach is most accurate when volatility jumps (whether dynamic or not) are present. That said, the five methods: BNS, CPR, MINRV, MEDRV and ASJ are all very similar, one to the other, in terms of their MSE^* values for any particular setting. In contrast, both PZ methods and, to a lesser extent, the ABD and LM methods, are relatively inaccurate in measuring the magnitude of a sequence of jumps. For example, the MSE^* values for the PZ2 and PZ4 approaches are more than about ten times the corresponding values for each of the five most accurate methods, for every specification documented in Tables 2 and 3. The rankings of the methods according to the clustering measures, $MSE^*_{\geq 2}$ and $MSE^*_{\geq 3}$, tally exactly with the rankings based on the overall MSE^*, for all jump specifications. This indicates that the relative accuracy of each method in constructing jump size measures is not sensitive to the precise manner in which sequences or clusters of jumps are defined.

Due to the reliance on the sign of the daily return in the construction of the price jump sign measure ($\overline{SCD^*}$), the sign measure for all but one of the approaches is identical for any given data generating process. The JO approach, which solves for the price jump size (and sign) from the nonlinear relation in (21), is the most accurate in detecting the *sign* when volatility jumps are absent (H1 and SD1), while the sign of the daily return serves better otherwise.

From these results we can deduce that no single approach produces the most accuracy across all seven measures. An approach that does well at detecting jumps may not perform well at measuring price jump magnitude, and vice versa. However, one *can* conclude that it is the CPR and MEDRV approaches that are most robust across *both* accuracy measure *and* price jump specification. These two approaches perform reasonably well at both detecting price jumps when present and not detecting absent jumps, in terms of accurately measuring the magnitude of the price jump, and in

terms of avoiding dependence in price jump detection errors. The BNS, which is arguably the most popular approach adopted in the literature, is also reasonably robust, but with accuracy measures that are consistently below those of CPR and MEDRV.[8]

4.3 Tuning parameter choice

As is clear from the outline of the jump test procedures in Section 2, all require a decision, of one form or another, to be made about the 'threshold' that is used to distinguish a continuous increment (dW_t^p) from a discontinuous increment (dJ_t^p) in (1). Such 'tuning' decisions clearly influence the values of the jump measures that are derived from the preliminary tests and, hence, any inferential results based on those measures. In all of the previous numerical exercises, we have employed a significance level of 1%, with the remaining tuning parameters specific to each test assigned the default values suggested by the authors. In this subsection, we discuss the impact of alternative choices for the significance level and certain other tuning values, prior to implementing some of these alternatives in the empirical investigation in Section 6. We divide the discussion into three segments, to aid the reader:

(i) *Significance level.* All tests are, of course, subject to the selection of a significance level, which determines the value beyond which the null hypothesis of 'no jump' is rejected. Tauchen & Zhou (2011) suggest the use of a 'small' significance level (in the range of 0.1% - 1%), based on their simulation study involving the BNS test. As noted earlier, ABD suggest a value of 0.001% to offset the size distortion associated with the multiple testing feature of their procedure. However, there does not appear to be widespread consensus in the literature regarding the choice of the significance level for the other tests. It is important to recognize that use of a higher level of significance will automatically lead to the identification of a greater number of apparent 'jumps', including those having a relatively small magnitude, according to the usual trade-off between the size of a test and its power in a neighbourhood of the null hypothesis of no jump. Thus, if the desired focus is to detect (and subsequently measure) jumps with reasonably large magnitude only, then a small significance level should be selected. In Section 6 we document inferential results based on significance levels of 0.1%, 0.5% and 1% for the three preliminary tests used therein (BNS, CPR and MEDRV) to produce the jump measures.

(ii) *Threshold value.* The higher-order $\mathcal{P}$-power variation-based ASJ and PZ tests, along with the CPR test, also entail the choice of certain threshold values that determine the particular jump-free variations that are accumulated. That is, these threshold values determine whether an individual return belongs to the diffusive component or to the jump component in the

[8] We also conducted this Monte Carlo assessment under different parameter settings from those documented in Table 1, including cases where the leverage effect is present, with $corr(dW_t^p, dW_t^v) < 0$. The magnitude of the accuracy measures do change, with accuracy tending to reduce with an increase in the average volatility jump size, as well as with a decrease in the signal-to-noise ratio. Nonetheless, the ranking amongst the approaches remains robust to the changes in parameter values.

calculation of $\mathcal{P}$-power variation. The thresholds for these tests are selected as a multiple of the local volatility estimate. For example, CPR suggest truncating returns at three times the local volatility measure. The choice of this multiplier ($c_\vartheta = 3$) is guided by the properties of a normal distribution, since if a jump is indeed absent, then the return (assumed to be normally distributed by approximation of the diffusive process) should cross the threshold only about 0.3% of the time. Naturally, a smaller multiplier will correspond to a larger proportion of returns being considered as part of the jump contribution. The ASJ and PZ tests prescribe truncations that involve the choice of the truncation root, ϖ. In both cases, a larger value of ϖ corresponds to a smaller level of the actual truncation point, again implying that a larger proportion of returns are considered as part of the jump contribution. With the CPR-based measures forming part of the empirical exercise in Section 6, we document inferential results therein based on $c_\vartheta = 3$, 4 and 5.

(iii) *Value of* $\mathcal{P}$. The $\mathcal{P}$-power variation-based tests are also subject to the choice of $\mathcal{P}$ itself, noting that, at least asymptotically, the jump contribution will dominate for values of $\mathcal{P} > 2$. However, with limited intra-day sampling available, a larger value of $\mathcal{P}$ will tend to accentuate jumps with relatively large magnitude and thereby diminishing the role in the test outcome of relatively small jumps, for any given choice of significance level. We refer the reader to the discussion in Section 2.2.

5 Implied inference about price jump dynamics: Artificial data

5.1 Data generation and model specification

The implications for *inference* - and in particular inference about the nature of price jumps - when using different approaches to produce the relevant jump measures, is now assessed in a simulation setting. We perform this assessment by generating data from the bivariate jump diffusion defined by (22) to (24), with the price jump intensity (δ_t^p) following the dynamic Hawkes process in (25) over $T = 2000$ trading days. To keep this particular exercise manageable, we impose $\delta^v = 0$, such that the volatility process has no jump component. The primary aim is then to gauge the robustness, or otherwise, of inference to the use of different high frequency measures (and associated preliminary tests) and to link - where feasible - inaccuracy in test outcomes and/or subsequent measurement to inferential inaccuracy, in a setting in which the true values of the parameters are known. In the empirical analysis in Section 6 we allow volatility to have, not only jumps, but jumps that evolve dynamically, in addition to the dynamic process allowed for price jumps.

As per the description in Section 4.1, data is simulated using a fine Euler discretization, with 720 observations created per trading day, equivalent to generating price observations every 30 seconds; the difference here being that the (discretized) Hawkes process for δ_t^p also plays a role in data generation, and volatility jumps are excluded. The price jump test statistics, and associated jump measures of occurrence, magnitude and sign, plus measures of integrated variance, are then

constructed using every 10^{th} observation over the daily interval, equivalent to a five-minute sampling frequency. We focus on *four* approaches only at this point: CPR and MEDRV, as the most robust approaches overall, according to the simulation results reported in Section 4.2.3; BNS, as the approach most commonly used in empirical studies; and ASJ, which is most accurate in terms of (sequential) jump magnitude measurement, but arguably the least accurate in terms of (sequential) jump detection.

The continuous-time model assumed to underlie the observed data is then discretized to the daily level, with only a single price jump allowed to occur on one day. This discrete-time model is estimated using a Bayesian simulation scheme, with marginal posterior means (MPMs) and 95% highest probability density (HPD) intervals compared with the true values for all parameters, as a method of gauging inferential accuracy. Particular attention is given to the accuracy with which the jump-related parameters are estimated, and the impact on that accuracy of either allowing for measurement error in the jump measures, or not doing so. As the model to be estimated is a version of the discrete state space model used in the empirical analysis in Maneesoonthorn *et al.* (2017), in which volatility jumps (that were a focus of that paper) are omitted and an additional measurement equation related to the sign of the price jump is introduced, the Markov chain Monte Carlo (MCMC) algorithm used therein is simply adapted to cater for these modifications, and we refer readers to that paper for details of the base algorithm. The model is also a slightly simplified version of the model that is estimated in Section 6 using empirical data on the S&P500 stock index and IBM stock prices.

With the time interval, $\Delta t = 1$, denoting a trading day, and $r_t = \ln P_{t+1} - \ln P_t$ defined as the log return over the day, the model to be estimated here comprises a collection of five measurement equations:

$$r_t = \mu + \gamma V_t + \sqrt{V_t}\xi_t^p + Z_t^p \Delta N_t^p \tag{32}$$

$$\ln \widehat{IV}_{*,t} = \psi_0 + \psi_1 \ln V_t + \sigma_{BV}\xi_t^{BV} \tag{33}$$

$$I_{*,t}^p = \begin{cases} Bernoulli\,(b) & \text{if } \Delta N_t^p = 1 \\ Bernoulli\,(a) & \text{if } \Delta N_t^p = 0 \end{cases} \tag{34}$$

$$\widetilde{M}_{*,t}^p = M_t^p + \sigma_{M_p}\xi_t^{M_p} \quad \text{for } RV_t > \widehat{IV}_{*,t} \tag{35}$$

$$\widetilde{S}_{*,t}^p = \begin{cases} \{-1,+1\} & \text{with probabilities } \{s_n, 1-s_n\} \text{ if } S_t^p = -1 \\ \{-1,+1\} & \text{with probabilities } \{s_p, 1-s_p\} \text{ if } S_t^p = +1 \end{cases} \tag{36}$$

five stochastic state equations:

$$V_{t+1} = \kappa\theta + (1-\kappa)\,V_t + \sigma_v\rho\,(r_t - Z_t^p\Delta N_t^p - \mu - \gamma V_t) + \sigma_v\sqrt{(1-\rho^2)\,V_t}\xi_t^v \tag{37}$$

$$\Delta N_t^p \sim Bernoulli(\delta_t^p) \tag{38}$$

$$Z_t^p = S_t^p \exp\,(M_t^p) \tag{39}$$

$$S_t^p = \begin{cases} -1 & \text{with probability } \pi_p \\ +1 & \text{with probability } (1-\pi_p) \end{cases} \tag{40}$$

$$M_t^p \sim N\left(\mu_p, \sigma_p^2\right) \tag{41}$$

with $\left(\xi_t^p, \xi_t^{BV}, \xi_t^{M_p}, \xi_t^v\right)' \sim N(0, I_{4\times 4})$, and a single conditionally deterministic, self-exciting, state equation:

$$\delta_t^p = \alpha_p \delta_\infty^p + (1-\alpha_p)\,\delta_{t-1}^p + \beta_p \Delta N_{t-1}^p \tag{42}$$

that is a discretized version of (25).

The two measures, $\widehat{IV}_{*,t}$ and $I_{*,t}^p$, in (33) and (34), respectively, are constructed from five-minute (simulated) returns, and linked to the relevant latent processes, as follows. The estimate of integrated variance, $\widehat{IV}_{*,t}$, is given by BV_t for the BNS approach, $CTBV_t$ for the CPR approach, $MedRV_t$ for the MEDRV approach, and by the truncated integrated variation in (11) with $\mathcal{P} = 2$ for the ASJ approach. From (33) it is seen that $\ln \widehat{IV}_{*,t}$ is treated as a noisy and potentially biased estimate of log integrated variance, with the latter represented by the logarithm of the end-of-day latent variance V_t; see also Koopman and Scharth (2013), Maneesoonthorn *et al.* (2012) and Maneesoonthorn *et al.* (2017). The jump occurrence measure, $I_{*,t}^p$, is computed as per (19), with $T_{*,t}$ and $C_*(\alpha)$ defined according to each of the four approaches. $I_{*,t}^p$ is viewed as a noisy measure of the latent price jump indicator in (38), with constant probabilities a and b to be estimated from the data. These latter two parameters can be viewed as a model-based representation of, respectively, the size and power of the test that underpins the measure $I_{*,t}^p$. We return to this interpretation in the empirical illustration in Section 6.

The logarithmic jump magnitude and jump sign measures, $\widetilde{M}_{*,t}^p$ and $\widetilde{S}_{*,t}^p$, (also constructed from the five-minute returns) are linked to the latent processes as follows. From (39) to (41) (which are, of course a restatement of (28) to (30), but with the subscript t now explicitly representing day t) the latent jump size, Z_t^p, is comprised of two components, the magnitude, $\exp(M_t^p)$, and the sign, S_t^p. The logarithm of the magnitude, M_t^p, is assumed to be Gaussian, with noisy measure $\widetilde{M}_{*,t}^p$. This measure is computed by taking the logarithm of the absolute value of the *signed* jump size measure, $\widetilde{Z}_{*,t}^p$, so that the sign (equated for all four of these approaches to the sign of the daily return) is removed.[9] This then allows the observed sign of the daily return, $\widetilde{S}_{*,t}^p$, to be viewed (separately) as a noisy measure of the true, but latent sign, S_t^p, as per (36). The measure $\widetilde{S}_{*,t}^p$ correctly detects a negative sign with probability s_n, and correctly detects a positive sign with probability $1 - s_p$. We also investigate the implications of using $I_{*,t}^p$, $\widetilde{M}_{*,t}^p$ and $\widetilde{S}_{*,t}^p$, as *exact* representations of ΔN_t^p, M_t^p and S_t^p, respectively; i.e. by re-estimating the model with an MCMC algorithm that treats these three latent jump components as being observed without error.

Finally, we note that, again in common with the empirical analysis undertaken in Maneesoonthorn *et al.* (2017), a combination of noninformative and weakly informative priors for the various unknown parameters are adopted. Certain details can be found in Appendix A of that paper, with the full prior specification documented in the on-line Supplementary Appendix of the current paper. Importantly, whilst this has not been documented in a formal way here, some preliminary

[9] Note that when the relevant $\widetilde{Z}_{*,t}^p$ equals zero, which happens when RV_t is less than or equal to the relevant measure of integrated variance, we do not view the data as providing any information about price jump size, and with $\widetilde{M}_{*,t}^p$ being undefined in this case.

investigations of the impact of the prior specification on the numerical results recorded below has been undertaken, with reasonable modifications to the base priors not found to exert any qualitative impact on the results.

5.2 Numerical results

Table 4 records the MPMs and HPD intervals for all parameters of the model specified in equations (32)-(42), with the true values recorded in the first column of the table. Due to the nature of the exercise, with the four nonparametric measures, $\widehat{IV}_{*,t}$, $I^p_{*,t}$, $\widetilde{M}^p_{*,t}$ and $\widetilde{S}^p_{*,t}$, having been constructed directly from the high frequency data, and then used as 'observed' measures in the relevant measurement equations, (33) to (36), the parameters of these four equations, ψ_0, ψ_1, σ_{BV}, b, a, σ_{M_p}, s_n and s_p, are simply estimated from the data, with there being no reference to 'true values'. The parameter estimates are reported in accordance with annualized returns expressed as proportions of one.

As is clear, the MPMs are all quite close to the corresponding true parameters and the latter fall within the 95% HPD intervals in most cases. One could deduce from this overall result that inference - in this form of model at least - is reasonably robust to the use of different high frequency measures/tests: an encouraging result for practitioners! Nevertheless, there *are* certain qualifications to this overall conclusion. For a start, the estimates (both point and interval) of the average jump size (μ_p) produced using the CPR and ASJ measures, substantially *under*estimate the true value. Simultaneously, these two measures produce point estimates that *over*estimate the unconditional mean for the (discretized) Hawkes intensity process, δ^p_0, as given in (27). The HPD intervals produced using the ASJ measures, for both of these parameters, are also qualitatively larger than those produced using the BNS, CPR and MEDRV measures, as is that for the parameter governing self-intensity, β_p, while the point estimate of the latter yielded by the ASJ measures is markedly smaller than the true value.

The estimates of the parameters in the lower panel of Table 4 provide information regarding aspects of the measurement error implicit in each of the four nonparametric measures, and the extent to which this varies across the four approaches. Notably, for the BNS, CPR and MEDRV measures, $\ln \widehat{IV}_{*,t}$ is seen to be a relatively accurate measure of $\ln V_t$,, as the corresponding estimates of ψ_0 and ψ_1 are reasonably close to 0 and 1, respectively, although the BNS interval for ψ_1 technically just misses the mark. In contrast, the ASJ version of $\ln \widehat{IV}_{*,t}$ is far from its 'true' value, and also results in larger estimates of the measurement error standard deviation, σ_{BV}, (in terms of the magnitude of the point estimate and the upper bound of the interval estimate) than do the other three versions. On the other hand, the accuracy with which the ASJ version of $\widetilde{M}^p_{*,t}$ measures the logarithmic price jump size, M^p_t, is better than for the other three approaches. Most notably however, viewing b as the power with which $I^p_{*,t}$ detects jumps, the estimate of this parameter is markedly lower under the ASJ approach, than it is for the other three approaches. These results regarding the relative performance of the ASJ method are in line with the reported accuracy

measures in Table 2, in which this approach was seen to perform poorly in terms of detecting price jumps under a Hawkes process (i.e. its value of $\overline{DJ^*}$ is very low), but well in terms of measuring the magnitude of jumps that are correctly detected (i.e. its values of MSE^*, $MSE^*_{\geq 2}$ and $MSE^*_{\geq 3}$ are relatively small).

Table 5 records the MPMs and 95% HPD intervals when inference is undertaken assuming $\Delta N_t^p = I_{*,t}^p$, $M_t^p = \widetilde{M}_{*,t}^p$ and $S_t^p = \widetilde{S}_{*,t}^p$, for $t = 1, ..., T$; i.e. when no measurement error is accommodated in the measurement of (latent) jump occurrence, (log) magnitude and sign. The most notable contrast with the corresponding results in Table 4 is that in all cases except for CPR, the measures pick up fewer jumps than they should, resulting in point estimates of the true value of the unconditional price jump intensity δ_0^p that are too small, and interval estimates whose upper bound is also less than the true value. Only MEDRV manages to report an HPD for μ_p that contains its true value. The ASJ approach, in particular, produces both point and interval estimates of δ_0^p and μ_p that are acutely inaccurate, as well as yielding HPD intervals for the other jump parameters, μ_p, σ_p and π_p, that are considerably wider than is the case for the other three measures, as well as being wider than the corresponding intervals in Table 4. We also note that under the CPR and MEDRV approaches, the apparent accuracy of $\ln \widehat{IV}_{*,t}$ as a measure of $\ln V_t$, remains qualitatively unaffected by the change (between Tables 4 and 5) in the treatment of the jump measures, whereas no such robustness is observed for the ASJ approach, and to a lesser degree using the BNS measures, according to the point and interval estimates of ψ_0 and ψ_1.

With due consideration taken of the limited nature of this exercise (i.e. as based on a particular data generating process, and a single 'empirical' sample generated therefrom) it seems clear that not all approaches used for price jump detection and measurement result in equally reliable inference, with the ASJ method possibly the least reliable overall of the four methods considered. We further remark that despite the overall robustness of the results to the assumed presence, or not, of noise in price jump detection and measurement, the results do confirm that explicit accommodation of measurement error in the price jump measures (as well as in the volatility measure) *does improve* inferential accuracy, in particular as it pertains to the price jump process itself. The incorporation of measurement error also, of course, accommodates the possible impact of microstructure noise on the nonparametric measures that may still remain, despite the use of a five-minute sampling interval, and the reported simulation results regarding the robustness of test power to such noise when the five-minute interval is used. For both of these reasons, the adoption of a state space structure with measurement error would seem to be a sensible modelling decision, and we proceed with that choice in the following empirical illustration.

6 Implied inference about price jump dynamics: Empirical data

6.1 Data details and model specification

We now extend the model under consideration to one in which both price and volatility have dynamic jump components. Specifically, we modify (37) to include dynamic volatility jumps, as in Maneesoonthorn *et al.* (2017), with (37) replaced by the following specification:

$$V_{t+1} = \kappa\theta + (1-\kappa)\, V_t + \sigma_v \rho \left(r_t - Z_t^p \Delta N_t^p - \mu - \gamma V_t\right) + \sigma_v \sqrt{(1-\rho^2)\, V_t} \xi_t^v + \Delta N_t^v Z_t^v \tag{43}$$

$$\Delta N_t^v \sim Bernoulli(\delta_t^v) \tag{44}$$

$$Z_t^v \sim Exp(\mu_v). \tag{45}$$

The volatility jump intensity is modelled via a Hawkes process as

$$\delta_t^v = \alpha_v \delta_\infty^v + (1-\alpha_v)\, \delta_{t-1}^v + \beta_v \Delta N_{t-1}^v + \beta_{vp} \Delta N_{t-1}^p, \tag{46}$$

with β_{vp} capturing any potential impact of price jumps on the volatility jump process. In addition, we allow for the price jump size to be related to the underlying volatility, as in Maneesoonthorn *et al.*, and alter the price jump size specification in (41) by

$$M_t^p \sim N(\mu_p + \gamma_p V_t, \sigma_p^2), \tag{47}$$

For the reasons noted at the end of the previous section we proceed by assuming that the jump measures are observed with error.

We employ daily S&P500 index (SPX) and IBM stock returns, with the data ranging from 3 January 2005 to 10 May 2018. The trade price data for IBM are obtained from Thomsons Reuters Tick History via the SIRCA database.[10] For each asset, we extract the median price at the five-minute frequency to construct the realized variance, as well as the measures of integrated volatility, jump occurrence and jump size, using the BNS, CPR and MEDRV approaches. Given the relative inaccuracy associated with use of the ASJ measure in the previous section, plus the very poor power performance of the ASJ test in the presence of volatility jumps documented in Section 4.1, we have decided to omit this test (and associated measure) from this exercise. In order to gauge the effect of the tuning choices in constructing the jump measures, we conduct preliminary jump tests for all three frameworks using the 0.1%, 0.5% and 1% significance levels. We also conduct the CPR jump test using $c_\vartheta = 3$, 4 and 5.

6.2 Numerical results

6.2.1 Summary statistics

We begin by presenting - for both data sets - some selected summary statistics in Table 6: the mean, standard deviation, skewness and kurtosis of daily returns (Panel A); the mean, standard deviation,

[10] Percentage daily logarithmic returns (instead of annualized returns expressed as proportions) are used in this section to alleviate numerical issues that arise within the MCMC algorithm due to variance estimates that are numerically small and close to zero.

skewness and kurtosis of the relevant measure of integrated variance (Panel B); the sample mean of the jump detection indicator $I^p_{*,t}$ in (19) (Panel C); and the mean, standard deviation, skewness and kurtosis of the measure of jump size (Panel D). The jump detection statistics are presented for varying values of significance level, and the summary statistics for all CPR-based measures are presented for the three different values of c_ϑ.

The key messages to be gleaned from this table are that: 1) as accords with the effect of portfolio diversification, the average return on IBM stock is higher than for the index, but at the cost of a higher volatility, as measured both by the standard deviation of returns and the mean value of all measures of the integrated variance; 2) the index return exhibits larger (negative) skewness and kurtosis than the stock, which is linked, in turn, to a higher *mean* measure of jump size (for all measures); 3) the mean of $I^p_{*,t}$ increases, as expected, as the significance level increases, and is larger overall (for any given significance level) for the stock; 4) for both data sets the mean of the CPR-based $I^p_{*,t}$ decreases as the truncation parameter c_ϑ increases; however, the impact of c_ϑ on the mean of the associated measure of jump size is negligible; 5) the degree of *variation*, *skewness* and *kurtosis* in all jump size measures is substantially higher for the stock than the index, and more sensitive (overall) to the type of the measure, with a similar comment regarding sensitivity to measure applying to the measures of integrated variance.

We next discuss the impact of measure (and tuning) choice on inference, making reference to the summary statistics in Table 6 where necessary. To aid the reader we discuss the results for the S&P500 and IBM data in turn, and focus the discussion primarily on inferential results as they pertain to key parameters controlling the dynamic price jump process. Tables 7 and 8 record the MPMs and 95% HPD intervals for the S&P500 index data, while Tables 9 and 10 record the corresponding values for IBM stock returns. Results based on the BNS and MEDRV measures appear in Tables 7 and 9, whilst the CPR results for each data series are presented in Tables 8 and 10, respectively. For the BNS, MEDRV and (base-case; $c_\vartheta = 3$) CPR measures, we document parameter estimates based on the three different significance levels for the jump detection tests: 0.1%, 0.5% and 1%. We also produce results based on the CPR measure using truncation values of $c_\vartheta = 4$ and $c_\vartheta = 5$ (for the 1% significance level only). Due to the decision to omit the ASJ test/measurement method from the empirical illustration, the tuning choice (iii) that is relevant to it (as is referenced in Section 4.3) is not explored further here. The parameter estimates reported in this section relate to percentage daily returns and are not annualized.

6.2.2 S&P500 index returns

With reference to the left-hand-side panel in Table 7 we see that inference (i.e. both the magnitude of the MPM and the coverage of the 95% HPD interval) based on the BNS measure is reasonably robust to the choice of significance level, with an exception of inference on δ^p_0 (the unconditional jump intensity in (27)) using 0.1% significance. As is consistent with the results recorded in Table 6, smaller values of significance imply that fewer jumps are detected. BNS-based inference conducted

using the 0.5% significance level does indeed produce a lower MPM for δ_0^p than under the 1% level; however, the HPD intervals in both cases still substantially overlap. In contrast, inference conducted using the 0.1% significance level yields a *much* lower MPM for δ_0^p, coupled with an HPD interval that overlaps little with those produced under the other two levels of significance.

Now looking at the results on the right-hand-side panel in Table 7 we see that inferences based on the MEDRV measure are reasonably similar overall to those based on the BNS measure, but only for the highest level of significance of 1% (albeit with the MEDRV measure implying a wider HPD interval for δ_0^p). The MEDRV results based on 0.5% and 0.1% significance levels generate some parameter estimates that are quite different from the others recorded in the table. Most notably, the two measures generated by these choices of significance levels lead to *very* wide 95% HPD intervals for δ_0^p, indicating much uncertainty about the intensity with which price jumps occur. Inferences regarding the volatility process are also qualitatively different: indicating less persistence (larger values for κ), a higher unconditional value (larger values for θ), and larger variation (larger values for σ_v). In addition, the volatility jump is found to be absent (indicated by the extremely low estimates - point and interval - of δ_0^v in the final two columns of the table), leading to correspondingly nonsensical estimates of the volatility jump size (μ_v) that are in stark contrast with the estimates recorded throughout the remainder of the table.

Referencing now the results in the left-hand-side panel of Table 8, which relate to CPR with default choice $c_\vartheta = 3$, we make the comment that, the 1% significance results are very similar to the corresponding results for BNS and MEDRV. However, in this case we can go further and say that these same *qualitative* results continue to obtain, for all three levels of significance, and for the two alternative values of c_ϑ (recorded on the right-hand-side panel of the table). In particular, the CPR-based conclusions regarding the nature of the dynamic jump process (represented by the estimates of all parameters subscripted by p) are robust to tuning parameter choice. That is, even though a decrease in significance level and/or an increase in c_ϑ cause the anticipated decline in δ_0^p, this decline is not substantial and, moreover, the associated changes in the parameters in (47) are very small. We also note that, and as is consistent with the results recorded in Section 4.1 in which the CPR jump test was found to have reasonable size and power properties in the presence of volatility jumps, the CPR-based estimates assign non-negligble values to *both* the price and volatility jump parameters, for all tuning choices.

Finally, for all measures we can make a link between the estimates of b and the estimated means of price jump size and volatility jump size, and the power curves presented in Figure 1. For example, with reference to the first column of results (MPM) in Table 8, the CPR measure based on a 1% significance level and $c_\vartheta = 3$ implies an average annualized price jump size[11] of 0.5 and an average volatility jump size[12] of 0.04. For this pair of tuning values, the CPR-based point estimate of b - viewed, as noted earlier, as a model-based representation of jump test power - is 0.780.

[11] Computed as $\exp(MPM(\mu_p) + MPM(\gamma_p) \times MPM(\theta + \delta_0^v \mu_v/\kappa)) \times 252/100^2$.
[12] Computed as $MPM(\mu_p) \times 252/100^2$.

Referencing Panel B of Figure 1, produced under the same tuning choices, we see that these three parameter estimates fit with the corresponding values on the power surface. A similar comment can be made about the relevant estimates and power surfaces for the BNS and MEDRV measures, noting, however, the extremely wide HPD interval of b from the MEDRV measure. This provides support for the reliability of all such measures in the given inferential setting. Furthermore, for all BNS and CPR results recorded in Tables 7 and 8, we observe a uniform decrease in the estimate of power (b) as the significance level of the jump test declines, as is consistent with the power/size trade-off that characterizes any application of hypothesis testing. This anticipated outcome is not, however, replicated for the results based on the MEDRV measure.

To conclude, it would appear that for the S&P 500 data - or data with characteristics that are broadly similar - the CPR measure is, overall, the method of choice, given its consistency with anticipated results regarding test power, its robustness to tuning parameter choice, and the fact that - in no one case - does it produce results that are starkly different from the results produced by an alternative measure. The key conclusions to be drawn from the CPR-based estimates are that both price and volatility jumps characterize the S&P500 data over this period, that both jump processes are indeed dynamic, and that price jumps do not have a (numerically) substantial influence on the volatility jump intensity; results that tally with earlier related work (Maneesoonthorn *et al.*, 2017).

6.2.3 IBM stock returns

Now referencing the results in Tables 9 and 10 for the IBM stock returns, we draw the following conclusions. First, the robustness of the BNS measure to tuning parameter choice mimics that seen for the index returns. That is, parameter inference based on the BNS measure is relatively robust to the choice of significance level, with the exception being inference on δ_0^p using the 0.1% level. We note, once again, the striking robustness of the CPR measure, across both significance level and the value of truncation parameter, c_ϑ. Viewing the results on the right-hand-side panel of Table 9, we see that the MEDRV measure provides more robust inference than was the case with the S&P500 returns, with the results at each significance level being in line with inference produced via the BNS and CPR measures. As is expected, and as is in line with the summary statistics summarized in Table 6, the MEDRV-based MPM of δ_0^p decreases with the level of significance, with the HPD intervals overlapping for the 1% and 0.5% levels of significance, but not for the 0.1% level.

Comparing the parameter estimates for IBM and the S&P500 index, the differences in the characteristics of these two financial assets are highlighted. First, as is consistent with the sample variance of returns and sample mean of the IV measures reported in Table 6, the unconditional variance of IBM is uniformly larger than that of the S&P500 index, given the larger estimates of θ, as well as the larger estimates of: the unconditional mean of the volatility jump intensity (δ_0^v) and the mean volatility jump size (μ_v). Second, the diffusive variance of the S&P500 returns is much more persistent than that of IBM, with estimates of κ that are significantly smaller.[13]. We

[13]This is in line with previous studies which have found the stochastic volatility process of the IBM to be less

also find that volatility jumps in the IBM returns occur much more frequently (larger δ_0^v), with a larger degree of self-excitation (larger β_v), despite the two assets' price jump intensities exhibiting similar time series dynamics. Finally, for IBM the expected decline in the 'power' parameter b as the significance level of the test declines is consistent across all measures, and the link between the relevant empirical estimates and the power surfaces in Figure 1 obtains for all cases also.

For this particular dataset then, the choice between measures is not quite as clear-cut; however, overall, the CPR measure is arguably still the best choice, due to its marked robustness to tuning value choice, in particular. Based on the CPR results, dynamic price and volatility jumps are seen to also characterize the IBM data over this period, with price jumps, once again, not substantially influencing the volatility jump intensity.

7 Discussion and Guidelines for Practitioners

Inferential work undertaken in empirical finance settings is often aimed at characterizing the nature and magnitude of the various risks - including price jump risk - thought to play a role in the dynamics of financial markets. Understanding the potential for the choice of price jump test, and associated jump measure, to influence inferential conclusions is thus vital. This paper provides an extensive evaluation of the multitude of price jump tests, and corresponding jump size (and sign) measures, that are now available to practitioners. Robustness to volatility jumps, the ability to detect and measure sequences, and clusters, of dynamic jumps, and the implications for subsequent inference of adopting different test and measurement approaches, have been the primary focus.

Our simulation experiments reveal that the power of some price jump tests is not robust to the presence of volatility jumps, while other tests suffer serious size distortions in the presence of confounding jumps in the variance process. Of the four categories of price jump tests outlined in Section 2, those based on squared variation appear to be the most robust overall. The tests based on $\mathcal{P}$-power variation seem to be the most problematic, particularly in the presence of volatility jumps, with those based on standardized returns also giving reasonable performance only when volatility jump is absent. The accuracy of the various aspects of price jump occurrence, magnitude and sign measurement, have been investigated, with the CPR test of Corsi, Pirino and Renò (2010) and the MEDRV test of Andersen, Dobrev and Schaumburg (2012) identified as being the most robust overall.

The use of alternative measurements in an inferential setting has also been explored using both artificially simulated data and empirical data. In the artificial data scenario, in which the true values of the parameters are known, we find that accounting for measurement error in jump measures is important when attempting to accurately infer the features of dynamic price jumps, with the use of such measures to directly represent the relevant latent quantities without error leading to less precise estimates of certain parameters. Hence, the empirical illustration is conducted with error

persistent than other series; see, for example, Jaquier *et al.* (1994), albeit based on different model specifications from ours.

in the measures accommodated. Robustness of the empirical results to tuning parameter choice (specifically, the significance level and truncation level c_ϑ), plus the overall robustness of inferential conclusions to the choice of measure is investigated for two different sets of empirical data.

To conclude, we offer practitioners the following *guidelines*:

1. The ASJ is the most accurate measure in terms of (sequential) jump magnitude measurement, but arguably the least accurate in terms of (sequential) jump detection. Critically though it has the poorest power performance in the presence of volatility jumps, and has been shown to be unreliable in terms of implied inferential accuracy. Thus, if accurate inference regarding price jumps is the goal, most notably in a model in which volatility jumps feature, this method would not appear to be a good choice.

2. Whilst the MEDRV measure performs reasonably well in terms of both detection and measurement of jumps, the inferential results that it produces are somewhat sensitive to significance level choice, as well as sometimes differing from results produced by other measures.

3. On the other hand, the popular BNS and CPR measures, as well as being reasonably accurate in jump detection and measurement, produce inferences regarding both index and stock returns that are quite consistent one set with the other, as well as being robust to tuning parameter choice. Both measures have also displayed reasonable size and power properties in the presence of volatility jumps. Either method would thus be a reasonable choice.

4. The CPR measure, however, is most marked in terms of robustness to tuning, and for both forms of data. It serves then as our preferred method overall, and the procedure that we recommend to practitioners requiring reliable inference on dynamic jump processes for financial returns.

References

[1] Aït-Sahalia, Y., Cacho-Diaz, J. and Laeven, R.J.A. 2015. Modeling Financial Contagion Using Mutually Exciting Jump Processes. *Journal of Financial Economics*, 109: 224-249.

[2] Aït-Sahalia, Y. and Jacod, J. 2009. Testing for Jumps in a Discretely Observed Process. *The Annals of Statistics*, 37: 184-222.

[3] Andersen, T.G., Bollerslev, T. and Diebold, F.X. 2007. Roughing It Up: Including Jump Components in the Measurement, Modeling and Forecasting of Return Volatility. *The Review of Economics and Statistics*, 89: 701-720.

[4] Andersen, T.G., Bollerslev, T., Diebold, F.X. and Labys, P. 2003. Modelling and Forecasting Realized Volatility. *Econometrica*, 71: 579-625.

[5] Andersen, T.G., Bollerslev, T. and Dobrev, D. 2007. No-Arbitrage Semi-Martingale Restrictions for Continuous-Time Volatility Models Subject to Leverage Effects, Jumps and IID Noise: Theory and Testable Distributional Implications. *Journal of Econometrics*, 138: 125-180.

[6] Andersen, T.G., Bollerslev, T., Frederiksen, P. and Nielsen, M.O. 2010. Continuous-Time Models, Realized Volatilities, and Testable Distributional Implications for Daily Stock Returns. *Journal of Applied Econometrics*, 25: 233-261.

[7] Andersen, T.G., Dobrev, D. and Schaumburg, E. 2012. Jump-Robust Volatility Estimation using Nearest Neighbor Truncation. *Journal of Econometrics*, 169: 75-93.

[8] Bandi, F.M. and Renò, R. 2016. Price and Volatility Co-Jumps. *Journal of Financial Economics*, 119: 107-146.

[9] Bandi, F.M. and Russell, J.R. 2008. Microstructure Noise, Realized Variance, and Optimal Sampling. *The Review of Economic Studies*, 75: 339-369.

[10] Barndorff-Nielsen, O.E. and Shephard, N. 2002. Econometric Analysis of Realized Volatility and Its Use in Estimating Stochastic Volatility Models. *Journal of the Royal Statistical Society Series B*, 64: 253-280.

[11] Barndorff-Nielsen, O.E. and Shephard, N. 2004. Power and Bipower Variation with Stochastic Volatility and Jumps. *Journal of Financial Econometrics*, 2: 1-37.

[12] Barndorff-Nielsen, O.E. and Shephard, N. 2006. Econometrics of Testing for Jumps in Financial Economics Using Bipower Variation. *Journal of Financial Econometrics*, 4: 1-30.

[13] Bates, D.S. 1996. Jumps and Stochastic Volatility: Exchange Rate Processes Implicit in Deutsche Mark Options. *Review of Financial Studies*, 9: 69-107.

[14] Bates, D.S. 2000. Post-87 Crash Fears in the S&P 500 Futures Option Market. *Journal of Econometrics*, 94: 181-238.

[15] Bollerslev, T., Kretschmer, U., Pigorsch, C. and Tauchen, G. 2009. A Discrete-Time Model for Daily S&P 500 Returns and Realized Variations: Jumps and Leverage Effects. *Journal of Econometrics*, 150: 151-166.

[16] Busch, T., Christensen, B.J. and Nielsen, M.O. 2011. The Role of Implied Volatility in Forecasting Future Realized Volatility and Jumps in Foreign Exchange, Stock, and Bond Markets, *Journal of Econometrics*, 160: 48-57.

[17] Chan, W.H. and Maheu, J.M. 2002. Conditional Jump Dynamics in Stock Market Returns. *Journal of Business and Economic Statistics*, 20: 377-389.

[18] Christensen, K., Oomen, Roel, C.A. and Podolskij. Mark, 2014. Fact or Friction: Jumps at Ultra High Frequency. *Journal of Financial Economics*, 114, 576-599.

[19] Christoffersen, P. F. 1998. Evaluating Interval Forecasts. *International Economic Review*, 39: 841-862.

[20] Corsi, F. 2009. A Simple Approximate Long Memory Model of Realized Volatility. *Journal of Financial Econometrics*, 7: 174-196.

[21] Corsi, F., Pirino, D. and Renò, R. 2010. Threshold Bipower Variation and the Impact of Jumps on Volatility Forecasting. *Journal of Econometrics*, 159: 276-288.

[22] Creal, D.D. 2008, Analysis of Filtering and Smoothing Algorithms for Levy-driven Stochastic Volatility Models. *Computational Statistics and Data Analysis*, 52: 2863-2876.

[23] Dobrev D, and Szerszen P. 2010. The Information Content of High-Frequency Data for Estimating Equity Return Models and Forecasting Risk. *Working paper*, SSRN.

[24] Duffie, D., Pan J. and Singleton, K. 2000. Transform Analysis and Asset Pricing for Affine Jump-Diffusions. *Econometrica*, 68: 1343-1376.

[25] Dumitru, A.M. and Urga, G. 2012. Identifying Jumps in Financial Assets: A Comparison Between Nonparametric Jump Tests. *Journal of Business and Economic Statistics*, 30: 242-255.

[26] Eraker, B. 2004. Do Stock Prices and Volatility Jump? Reconciling Evidence from Spot and Option Prices. *The Journal of Finance*, LIX: 1367-1403.

[27] Eraker, B., Johannes, M. and Polson, N. 2003. The Impact of Jumps in Volatility and Returns. *The Journal of Finance*, LVIII: 1269-1300.

[28] Fulop, A., Li, J. and Yu, J. 2014. Self-Exciting Jumps, Learning, and Asset Pricing Implications. *Review of Financial Studies*, 28: 876-912.

[29] Hansen, P.R., Huang, Z. and Shek, H.H. 2012. Realized GARCH: A Joint Model for Returns and Realized Measures of Volatility. *Journal of Applied Econometrics*, 27: 877-906.

[30] Hansen, P.R. and Lunde, A. 2006. Realized Variance and Market Microstructure Noise. *Journal of Business and Economic Statistics*, 24: 127-161.

[31] Hawkes, A.G. 1971a. Spectra of Some Self-Exciting and Mutually Exciting Point Processes. *Biometrika*, 58: 83-90.

[32] Hawkes, A.G. 1971b. Point Spectra of Some Mutually Exciting Point Processes. *Journal of the Royal Statistical Society: Series B (Statistical Methodology)*, 33: 438-443.

[33] Huang, X. and Tauchen, G. 2005. The Relative Contribution of Jumps to Total Price Variance. *Journal of Financial Econometrics*, 3: 456-499.

[34] Jacquier E., Polson, N.G. and Rossi, P.E. 1994. Bayesian Analysis of Stochastic Volatility Models. Journal of Business and Economic Statistics, 12: 69-87.

[35] Jiang, G.J. and Oomen, R.C. 2008. Testing for Jumps When Asset Prices are Observed with Noise: A 'Swap Variance' Approach. *Journal of Econometrics*, 144: 352-370.

[36] Koopman, S. J., Jungbacker, B. and Hol, E. 2005. Forecasting Daily Variability of the S&P100 Stock Index using Historical, Realized and Implied Volatility Measurements, *Journal of Empirical Finance*, 12: 445-475.

[37] Koopman, S.J. and Scharth, M. 2013. The Analysis of Stochastic Volatility in the Presence of Daily Realized Measures. *Journal of Financial Econometrics*, 11: 76-115.

[38] Lee, S.S. and Mykland, P.A. 2008. Jumps in Financial Markets: A New Nonparametric Test and Jump Dynamics. *Review of Financial Studies*, 21: 2535-2563.

[39] Maheu, J.M. and McCurdy, T.H. 2004. News Arrival, Jump Dynamics, and Volatility Components for Individual Stock Returns. *The Journal of Finance*, LIX: 755-793.

[40] Maneesoonthorn, W., Forbes, C.S. and Martin, G.M. 2017. Inference on Self-Exciting Jumps Using High-Frequency Measures. *Journal of Applied Econometrics*, 32: 504-532.

[41] Maneesoonthorn, W., Martin, G.M., Forbes, C.S. and Grose, S. 2012. Probabilistic Forecasts of Volatility and its Risk Premia. *Journal of Econometrics*, 171: 217-236.

[42] Martin, G.M., Reidy, A.R. and Wright, J. 2009. Does the Option Market Produce Superior Forecasts of Noise-Corrected Volatility Measures? *Journal of Applied Econometrics*, 24: 77-104.

[43] Merton, R.C. 1976. Option Pricing When Underlying Stock Returns Are Discontinuous. *Journal of Financial Economics*, 3: 125-144.

[44] Neuberger, A. 1994. The Log Contract. *The Journal of Portfolio Management*, 20: 74-80.

[45] Pan, J. 2002. The Jump-risk Premia Implicit in Options: Evidence from an Integrated Time-series Study. *Journal Of Financial Economics*, 63: 3-50.

[46] Podolskij, M. and Ziggel, D. 2010. New Tests for Jumps in Semimartingale Models. *Statistical Infererence for Stochastic Processes*, 13: 15-41.

[47] Takahashi, M., Omori, Y. and Watanabe, T. 2009. Estimating Stochastic Volatility Models Using Daily Returns and Realized Volatility Simultaneously. *Computational Statistics and Data Analysis*, 53: 2404-2426.

[48] Tauchen G. and Zhou, H. 2011. Realized Jumps on Financial Markets and Predicting Credit Spreads. *Journal of Econometrics*, 160: 102-118.

[49] Todorov, V. 2010. Variance Risk-Premium Dynamics: The Role of Jumps. *Review of Financial Studies*, 23: 345-383.

[50] Todorov, V. and Tauchen, G. 2011. Volatility Jumps. *Journal of Business & Economic Statistics*, 29: 356-371.

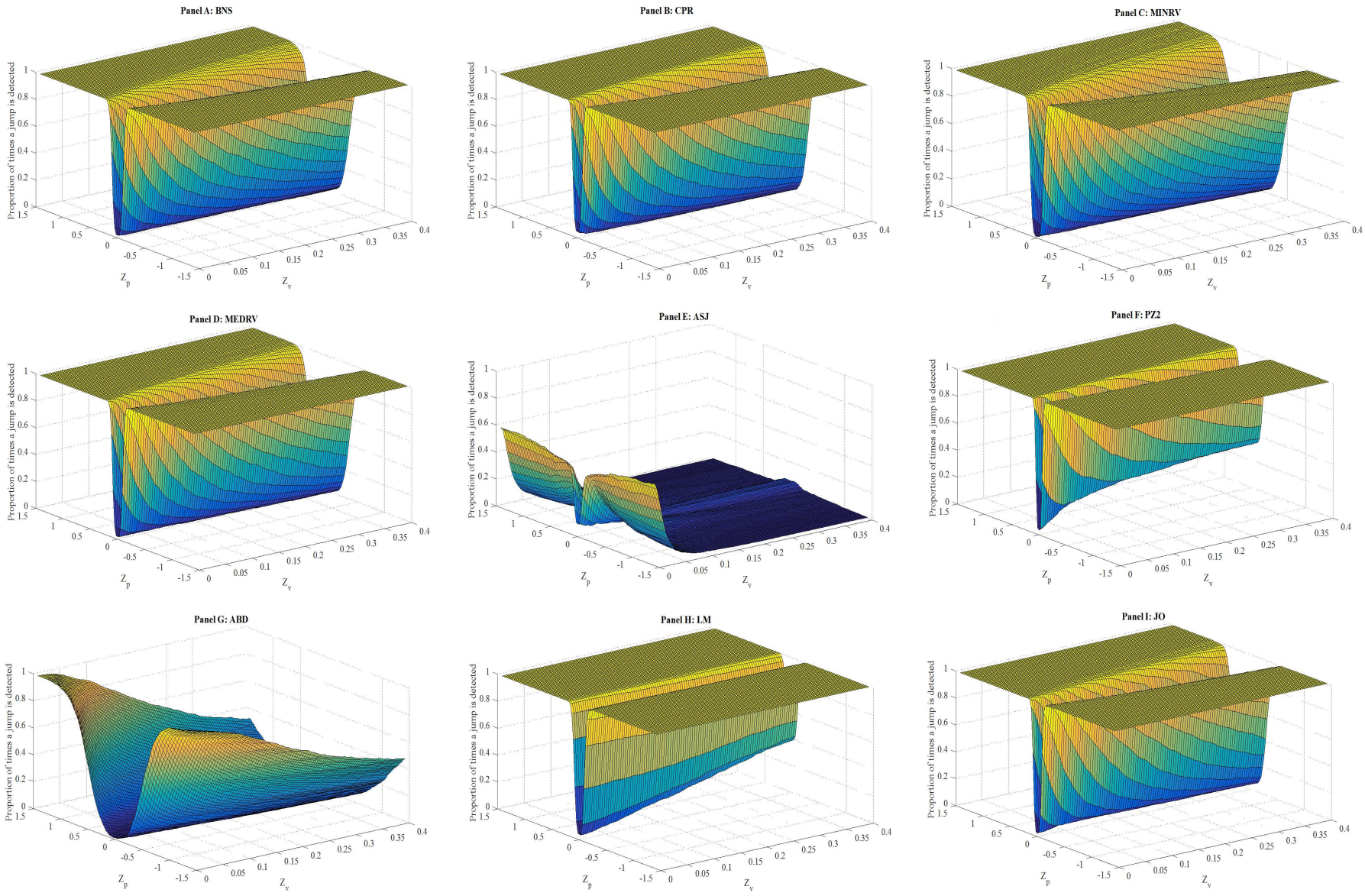

Figure 1: Power curves over changing price and volatility jump sizes (Z_p and Z_v, respectively).

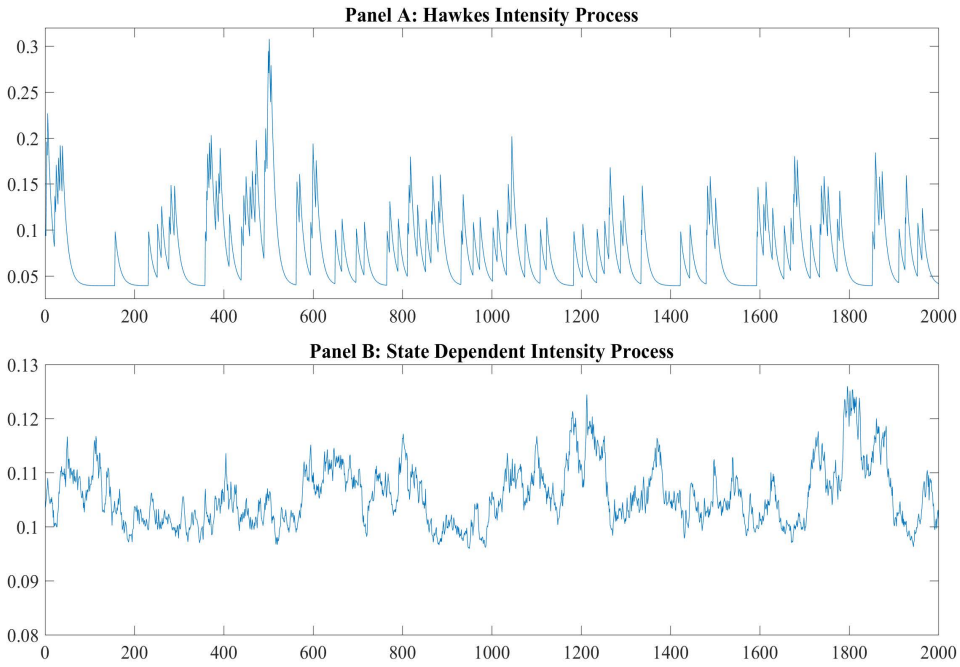

Figure 2: Panel A: the price jump intensity process implied by the Hawkes specification in (25); Panel B: the price jump intensity implied by the state dependent specification in (26). The realizations reproduced in both panels are based on the parameter values recorded in Table 1.

Table 1: True parameter values for the model components specified in (22)-(31). SD1 and H1 impose no volatility jumps. SD2 and H2 assume constant intensity volatility jumps independent of price jumps. SD3 and H3 also assume independent price and volatility jumps but with each sharing the same jump intensity process.

	SD1	SD2	SD3	H1	H2	H3
Panel A: Jump intensity settings						
δ_0^p	0.105	0.105	0.105	0.105	0.105	0.105
β_{p0}	0.100	0.100	0.100	–	–	–
β_{p1}	0.500	0.500	0.500	–	–	–
α_p	–	–	–	0.094	0.094	0.094
β_p	–	–	–	0.059	0.059	0.059
δ_0^v	0	0.105	0.105	0	0.105	0.105
β_{v0}	–	–	0.100	–	–	–
β_{v1}	–	–	0.500	–	–	–
α_v	–	–	–	–	–	0.094
β_v	–	–	–	–	–	0.059
Panel B: Jump size settings						
μ_p	1.00	1.00	1.00	1.00	1.00	1.00
σ_p	0.50	0.50	0.50	0.50	0.50	0.50
π_p	0.50	0.50	0.50	0.50	0.50	0.50
$\mu_v = 1.5 \times \theta$	0.03	0.03	0.03	0.03	0.03	0.03

Table 2: Accuracy measures for each price jump measurement framework under a bivariate jump diffusion for price and volatility, with the Hawkes process in (25) for the price jump intensity. In each column, the figure that is deemed the most favourable accuracy measure, under each of the three versions of the data generating process, is highlighted in bold. **Large** values are favoured for $\overline{DJ^*}$, $\overline{NDJ^*}$ and SCD^*; **small** values are favoured for SDE^*, MSE^*, $MSE^*_{\geq 2}$ and $MSE^*_{\geq 3}$.

		$\overline{DJ^*}$	$\overline{NDJ^*}$	SDE^*	MSE^*	$MSE^*_{\geq 2}$	$MSE^*_{\geq 3}$	$\overline{SCD^*}$
	BNS	0.816	0.986	0.089	0.411	0.386	0.373	0.885
	CPR	0.880	0.954	**0.046**	0.288	0.267	0.254	0.885
	MINRV	0.771	0.993	0.155	0.285	0.264	0.250	0.885
	MEDRV	0.853	0.988	0.069	0.268	0.245	0.229	0.885
H1	ASJ	0.043	0.998	0.749	**0.255**	**0.232**	**0.216**	0.885
	PZ2	0.952	0.976	0.070	12.082	12.149	12.073	0.885
	PZ4	0.861	**0.999**	0.074	12.082	12.149	12.073	0.885
	ABD	0.062	0.995	0.733	11.855	11.909	11.820	0.885
	LM	0.734	0.969	0.079	10.854	10.914	10.838	0.885
	JO	**0.980**	0.973	0.097	4.592	4.599	4.556	**0.908**
	BNS	0.339	0.986	0.417	1.778	1.785	1.835	**0.718**
	CPR	0.452	0.955	0.186	1.523	1.537	1.562	**0.718**
	MINRV	0.268	0.992	0.522	1.561	1.564	1.614	**0.718**
	MEDRV	0.379	0.988	0.411	**1.356**	**1.357**	**1.393**	**0.718**
H2	ASJ	0.033	**0.998**	0.770	1.448	1.450	1.493	**0.718**
	PZ2	**0.652**	0.960	**0.122**	17.099	17.198	17.178	**0.718**
	PZ4	0.601	0.985	0.243	17.099	17.198	17.178	**0.718**
	ABD	0.010	0.997	0.771	12.082	12.164	12.173	**0.718**
	LM	0.341	0.969	0.323	11.137	11.219	11.229	**0.718**
	JO	0.498	0.973	0.231	6.049	6.098	6.129	0.496
	BNS	0.403	0.986	0.4210	1.620	1.632	1.620	**0.740**
	CPR	0.513	0.955	0.1860	1.379	1.393	1.360	**0.740**
	MINRV	0.335	0.993	0.5580	1.423	1.423	1.408	**0.740**
	MEDRV	0.446	0.988	0.3990	**1.234**	**1.237**	**1.220**	**0.740**
H3	ASJ	0.035	**0.998**	0.7600	1.322	1.330	1.307	**0.740**
	PZ2	**0.696**	0.961	**0.1280**	16.919	17.025	17.186	**0.740**
	PZ4	0.634	0.987	0.2880	16.919	17.025	17.186	**0.740**
	ABD	0.014	0.996	0.7660	12.143	12.168	12.197	**0.740**
	LM	0.393	0.969	0.2880	11.176	11.209	11.251	**0.740**
	JO	0.559	0.973	0.2280	5.877	5.900	5.885	0.557

Table 3: Accuracy measures for each price jump measurement framework under a bivariate jump diffusion for price and volatility, with the state dependent process in (26) for the price jump intensity. In each column, the figure that is deemed the most favourable accuracy measure, under each of the three versions of the data generating process, is highlighted in bold. **Large** values are favoured for $\overline{DJ^*}$, $\overline{NDJ^*}$ and $\overline{SCD^*}$; **small** values are favoured for SDE^*, MSE^*, $MSE^*_{\geq 2}$ and $MSE^*_{\geq 3}$.

		$\overline{DJ^*}$	$\overline{NDJ^*}$	SDE^*	MSE^*	$MSE^*_{\geq 2}$	$MSE^*_{\geq 3}$	$\overline{SCD^*}$
	BNS	0.810	0.986	0.073	0.419	0.410	0.424	0.882
	CPR	0.876	0.954	0.046	0.295	0.285	0.291	0.882
	MINRV	0.765	0.993	0.069	0.292	0.285	0.300	0.882
	MEDRV	0.848	0.988	0.036	0.272	0.263	0.273	0.882
SD1	ASJ	0.044	0.998	0.057	**0.259**	**0.250**	**0.262**	0.882
	PZ2	**0.950**	0.976	0.064	12.163	12.068	11.667	0.882
	PZ4	0.859	**1.000**	**0.022**	12.163	12.068	11.667	0.882
	ABD	0.061	0.995	0.052	11.931	11.823	11.433	0.882
	LM	0.732	0.969	0.067	10.924	10.820	10.442	0.882
	JO	0.904	0.973	0.083	4.627	4.577	4.449	**0.903**
	BNS	0.311	0.986	0.078	1.917	2.023	2.156	**0.710**
	CPR	0.425	0.955	0.070	1.664	1.774	1.909	**0.710**
	MINRV	0.241	0.993	0.083	1.703	1.822	1.976	**0.710**
	MEDRV	0.349	0.988	0.085	**1.478**	**1.575**	**1.717**	**0.710**
SD2	ASJ	0.031	**0.998**	**0.054**	1.602	1.723	1.895	**0.710**
	PZ2	**0.625**	0.960	0.083	18.048	19.020	20.456	**0.710**
	PZ4	0.582	0.985	0.140	18.048	19.020	20.456	**0.710**
	ABD	0.008	0.997	0.056	12.116	12.194	12.566	**0.710**
	LM	0.316	0.969	0.074	11.192	11.283	11.621	**0.710**
	JO	0.469	0.973	0.096	6.210	6.364	6.653	0.468
	BNS	0.209	0.986	0.152	2.767	2.994	3.204	**0.671**
	CPR	0.305	0.955	0.140	2.595	2.835	3.092	**0.671**
	MINRV	0.150	0.993	0.149	2.732	2.989	3.223	**0.671**
	MEDRV	0.234	0.988	0.181	**2.348**	**2.568**	**2.774**	**0.671**
SD3	ASJ	0.023	**0.998**	0.074	2.718	3.003	3.289	**0.671**
	PZ2	**0.486**	0.960	0.156	26.930	29.223	31.513	**0.671**
	PZ4	0.466	0.975	0.244	26.930	29.223	31.513	**0.671**
	ABD	0.006	0.997	**0.072**	12.176	12.209	12.309	**0.671**
	LM	0.222	0.969	0.117	11.385	11.452	11.564	**0.671**
	JO	0.337	0.972	0.145	7.174	7.412	7.682	0.334

Table 4: Parameter inference when treating jump measures as observed with error. Under each form of measure (BNS, CPR, MEDRV and ASJ), we report the marginal posterior mean (MPM) and 95% highest posterior density (HPD) credible interval for each of the model parameters. The true parameter values used to generate the data are also reported. All true and estimated parameter values are reported in accordance with annualized returns represented as proportions of one. As noted in the text, true values for α, β, s_n, s_p, σ_{M_p}, ψ_0, ψ_1 and σ_{BV} are not specified.

		BNS		CPR		MEDRV		ASJ	
	True	MPM	95% HPD int	MPM	95% HPD int	MPM	95% HPD int	MPM	95% HPD int
μ	0.2	0.231	(0.126,0.334)	0.226	(0.116,0.328)	0.244	(0.139,0.345)	0.217	(0.101,0.333)
γ	-7.9	-5.903	(-9.771,-0.794)	-6.163	(-9.797,-0.820)	-6.450	(-9.826,-1.086)	-6.062	(-9.814,-0.837)
ρ	0.00	-0.018	(-0.086,0.046)	-0.013	(-0.079,0.060)	0.008	(-0.066,0.080)	0.008	(-0.062,0.080)
κ	0.03	0.023	(0.013,0.033)	0.023	(0.013,0.033)	0.022	(0.012,0.032)	0.034	(0.010,0.144)
θ	0.02	0.021	(0.016,0.028)	0.021	(0.016,0.027)	0.021	(0.016,0.029)	0.022	(0.014,0.030)
σ_v	0.02	0.019	(0.017,0.020)	0.019	(0.017,0.022)	0.018	(0.017,0.021)	0.023	(0.018,0.043)
μ_p	1.0	0.950	(0.783,1.099)	0.698	(0.526,0.842)	1.035	(0.874,1.178)	0.607	(0.399,0.911)
σ_p	0.5	0.457	(0.353,0.581)	0.531	(0.436,0.637)	0.449	(0.349,0.560)	0.586	(0.479,0.553)
π_p	0.5	0.497	(0.418,0.576)	0.474	(0.408,0.541)	0.487	(0.407,0.567)	0.471	(0.379,0.553)
δ_0^p	0.105	0.092	(0.073,0.117)	0.131	(0.107,0.167)	0.086	(0.069,0.108)	0.203	(0.069,0.491)
α_p	0.094	0.131	(0.061,0.219)	0.159	(0.069,0.233)	0.155	(0.074,0.234)	0.132	(0.028,0.219)
β_p	0.059	0.047	(0.021,0.077)	0.043	(0.017,0.072)	0.050	(0.022,0.083)	0.013	(4.8E-4,0.077)
ψ_0	–	-0.135	(-0.296,-0.005)	-0.116	(-0.265,0.008)	-0.264	(-0.420,-0.118)	-0.797	(-2.382,-0.114)
ψ_1	–	0.957	(0.916,0.993)	0.967	(0.929,1.000)	0.931	(0.887,0.971)	0.798	(0.424,0.995)
σ_{BV}	–	0.205	(0.196,0.214)	0.208	(0.198,0.218)	0.202	(0.191,0.211)	0.234	(0.163,0.624)
b	–	0.821	(0.657,0.950)	0.823	(0.646,0.948)	0.823	(0.667,0.949)	0.041	(9.4E-3,0.097)
a	–	7.7E-4	(1.8E-5,2.9E-3)	7.7E-4	(1.8E-5,3.0E-3)	7.7E-4	(1.9E-5,2.8E-3)	5.4E-4	(1.6E-5,2.0E-3)
σ_{M_p}	–	1.612	(1.434,1.773)	1.212	(1.029,1.372)	1.600	(1.425,1.759)	0.371	(0.269,0.573)
s_n	–	0.937	(0.873,0.979)	0.947	(0.895,0.983)	0.936	(0.871,0.978)	0.954	(0.879,0.992)
s_p	–	0.059	(0.019 ,0.118)	0.044	(0.015,0.091)	0.059	(0.020,0.117)	0.040	(7.1E-3,0.358)

Table 5: Parameter inference when treating jump measures as observed without error. Under each form of measure (BNS, CPR, MEDRV and ASJ), we report the marginal posterior mean (MPM) and 95% highest posterior density (HPD) credible interval for each of the model parameters. The true parameter values used to generate the data are also reported. All true and estimated parameter values are reported in accordance with annualized returns represented as proportions of one. Note that in this case, the parameters α, β, s_n, s_p, and σ_{M_p} are irrelevant as the price jump measures are treated as observed without error. As in Table 4, true values of ψ_0, ψ_1 and σ_{BV} are not specified.

		BNS		CPR		MEDRV		ASJ	
	True	MPM	95% HPD int	MPM	95% HPD int	MPM	95% HPD int	MPM	95% HPD int
μ	0.2	0.237	(0.131,0.335)	0.233	(0.131,0.333)	0.249	(0.146,0.345)	0.260	(0.137,0.376)
γ	-7.9	-6.087	(-9.782,-0.957)	-6.378	(-9.811,-1.050)	-6.830	(-9.879,-1.497)	-5.945	(-9.763,-0.723)
ρ	0.00	-0.028	(-0.097,0.043)	-0.018	(-0.091,0.055)	-0.004	(-0.074,0.063)	-0.002	(-0.066,0.061)
κ	0.03	0.022	(0.013,0.032)	0.023	(0.014,0.034)	0.022	(0.013,0.032)	0.023	(0.014,0.033)
θ	0.02	0.021	(0.017,0.028)	0.021	(0.016,0.027)	0.020	(0.016,0.026)	0.024	(0.019,0.031)
σ_v	0.02	0.019	(0.018,0.020)	0.019	(0.017,0.020)	0.017	(0.016,0.019)	0.020	(0.018,0.021)
μ_p	1.0	0.819	(0.738,0.901)	0.644	(0.565,0.721)	0.969	(0.894,1.045)	0.514	(-0.010,1.028)
σ_p	0.5	0.508	(0.456,0.570)	0.597	(0.545,0.657)	0.455	(0.405,0.511)	0.621	(0.399,1.016)
π_p	0.5	0.500	(0.422,0.578)	0.473	(0.409,0.538)	0.489	(0.411,0.566)	0.560	(0.323,0.784)
δ_0^p	0.105	0.076	(0.065,0.088)	0.108	(0.095,0.122)	0.072	(0.061,0.083)	0.004	(0.001,0.007)
α_p	0.094	0.134	(0.066,0.242)	0.170	(0.073,0.235)	0.173	(0.077,0.258)	0.193	(0.053,0.250)
β_p	0.059	0.048	(0.024,0.076)	0.045	(0.019,0.074)	0.052	(0.024,0.087)	0.029	(0.001 ,0.099)
ψ_0	–	-0.195	(-0.321,-0.045)	-0.107	(-0.310,0.040)	0.066	(-0.133,0.255)	-0.152	(-0.287,0.0175)
ψ_1	–	0.950	(0.915,0.991)	0.964	(0.907,1.003)	1.002	(0.948,1.054)	1.001	(0.963,1.049)
σ_{BV}	–	0.206	(0.197,0.215)	0.206	(0.197,0.216)	0.202	(0.192,0.212)	0.168	(0.159,0.177)

Table 6: Descriptive statistics for S&P500 and IBM daily percentage returns, and measures of integrated volatility, jump occurence and jump size. The sample period is from 3 January 2005 to 10 May 2018.

		SPX					IBM				
		BNS	CPR (c=3)	CPR (c=4)	CPR (c=5)	MEDRV	BNS	CPR (c=3)	CPR (c=4)	CPR (c=5)	MEDRV
Return	Mean			0.010					0.019		
	Stdev			0.879					0.933		
	Skew			-0.229					-0.119		
	Kurt			15.038					8.460		
Measure of IV	Mean	0.669	0.660	0.667	0.668	0.663	1.172	1.106	1.124	1.129	1.192
	Stdev	1.900	1.887	1.898	1.898	1.985	3.182	2.284	2.347	2.360	4.590
	Skew	10.075	10.238	10.097	10.091	11.160	20.442	8.505	8.656	8.584	35.098
	Kurt	140.737	145.771	141.185	141.139	176.783	681.242	102.178	105.670	103.657	1628.880
Jump Detection	1% Sig.	0.096	0.132	0.107	0.100	0.106	0.101	0.135	0.110	0.105	0.105
	0.05% Sig.	0.072	0.101	0.083	0.077	0.078	0.083	0.111	0.088	0.085	0.081
	0.01% Sig.	0.035	0.058	0.043	0.038	0.034	0.048	0.069	0.056	0.051	0.045
Jump Size Measure	Mean	0.011	0.011	0.011	0.010	0.012	0.006	0.009	0.010	0.009	0.002
	Stdev	0.231	0.248	0.236	0.233	0.260	0.364	0.444	0.424	0.418	0.389
	Skew	0.290	0.087	0.305	0.272	0.356	0.945	6.302	6.853	6.981	-0.204
	Kurt	13.929	14.415	13.556	13.833	10.725	30.126	176.758	200.045	204.470	11.946

Table 7: Pecentage daily S&P500 index returns between 3 Jan 2005 and 10 May 2018. Estimation of the dynamic jump model defined by (32)-(36), (38)-(40) and (42)-(47), with jump measurement errors included. The jump measures are constructed using the BNS and MEDRV frameworks, each under the significance levels of 1%, 0.5% and 0.1%. We report the marginal posterior mean (MPM) and 95% highest posterior density (95% HPD) credible interval for each of the model parameters.

	BNS						MEDRV					
	1% significance		0.5% significance		0.1% significance		1% significance		0.5% significance		0.1% significance	
	MPM	95% HPD Interval	MPM	95% HPD Interval	MPM	95% HPD Interval	MPM	95% HPD Interval	MPM	95% HPD Interval	MPM	95% HPD Interval
μ	0.062	(0.026,0.102)	0.064	(0.026,0.105)	0.064	(0.029,0.104)	0.064	(0.024,0.103)	0.124	(-0.013,1.121)	0.073	(0.016,0.119)
γ	-0.070	(-0.130,-0.016)	-0.068	(-0.129,-0.014)	-0.064	(-0.122,-0.013)	-0.076	(-0.137,-0.017)	-0.198	(-0.266,-0.004)	-0.136	(-0.090,-0.005)
ρ	-0.351	(-0.446,-0.245)	-0.361	(-0.459,-0.256)	-0.367	(-0.459,-0.264)	-0.336	(-0.435,-0.229)	-0.177	(-0.355,0.585)	-0.241	(-0.384,-0.124)
κ	0.047	(0.025,0.076)	0.050	(0.025,0.076)	0.052	(0.027,0.078)	0.046	(0.024,0.078)	0.176	(0.051,0.953)	0.090	(0.034,0.309)
θ	0.461	(0.365,0.571)	0.456	(0.356,0.569)	0.447	(0.350,0.552)	0.477	(0.332,0.590)	1.930	(0.989,9.180)	1.589	(1.056,2.090)
σ_v	0.115	(0.102,0.129)	0.117	(0.103,0.132)	0.117	(0.105,0.131)	0.115	(0.101,0.130)	0.692	(0.426,2.980)	0.457	(0.288,0.754)
μ_p	-2.246	(-2.297,-2.199)	-2.236	(-2.285,-2.185)	-2.230	(-2.278-2.181)	-2.125	(-2.177,-2.063)	-1.985	(-2.163,-1.896)	-1.986	(-2.034,-1.932)
γ_p	0.490	(0.405,0.579)	0.470	(0.382,0.553)	0.461	(0.362,0.536)	0.502	(0.407,0.589)	0.175	(0.131,0.222)	0.183	(0.155,0.223)
σ_p	0.436	(0.362,0.502)	0.436	(0.364,0.498)	0.433	(0.359,0.503)	0.447	(0.363,0.528)	0.494	(0.387,0.601)	0.470	(0.389,0.547)
π_p	0.331	(0.156,0.524)	0.318	(0.140,0.533)	0.339	(0.131,0.594)	0.331	(0.160,0.522)	0.379	(0.054,0.951)	0.395	(0.111,0.692)
δ_0^p	0.115	(0.063,0.169)	0.084	(0.035,0.135)	0.039	(0.007,0.074)	0.139	(0.051,0.461)	0.237	(0.003,0.969)	0.050	(9.28E-4,0.39)
α_p	0.223	(0.066,0.263)	0.119	(0.017,0.232)	0.161	(0.046,0.2409)	0.153	(0.023,0.233)	0.131	(0.033,0.214)	0.150	(0.036,0.227)
β_p	0.019	(0.003,0.045)	0.013	(0.001,0.034)	0.024	(0.004,0.055)	0.011	(6.95E-4,0.032)	0.012	(0.001,0.040)	0.018	(0.001,0.059)
μ_v	1.613	(0.800,2.977)	1.544	(0.882,2.922)	1.520	(0.822,3.228)	1.984	(0.874,5.140)	1.80E76	(2.4E33,6.5E76)	3.38E50	(2.26E8,2.09E51)
δ_0^v	0.020	(0.007,0.043)	0.022	(0.009,0.040)	0.024	(0.009,0.049)	0.017	(0.006,0.045)	2.91E-4	(7.20E-6,0.001)	3.73E-4	(8.39E-6,0.001)
α_v	0.151	(0.016,0.523)	0.137	(0.015,0.727)	0.087	(0.015,0.511)	0.218	(0.018,0.661)	0.561	(0.239,0.753)	0.733	(0.322,0.802)
β_v	0.025	(0.004,0.066)	0.025	(0.005,0.066)	0.023	(0.006,0.054)	0.028	(0.003,0.080)	0.142	(0.006,0.330)	0.139	(0.006,0.270)
β_{vp}	0.003	(5.16E-5,0.015)	0.003	(2.52E-5,0.014)	0.003	(3.85E-5,0.017)	0.003	(6.79E-5,0.013)	0.003	(1.02E-5,0.017)	0.010	(5.85E-5,0.056)
ψ_0	-0.664	(-0.789,-0.552)	-0.678	(-0.804,-0.569)	-0.680	(-0.831,-0.584)	-0.681	(-0.815,-0.576)	-1.275	(-2.144,-1.045)	-1.187	(-1.374,-1.020)
ψ_1	1.289	(1.160,1.395)	1.277	(1.145,1.387)	1.272	(1.089,1.371)	1.326	(1.154,1.444)	0.904	(0.722,1.131)	0.932	(0.842,1.046)
σ_{BV}	0.546	(0.506,0.596)	0.544	(0.507,0.595)	0.542	(0.507,0.601)	0.558	(0.515,0.631)	0.728	(0.598,1.044)	0.631	(0.559,0.788)
b	0.737	(0.497,0.935)	0.715	(0.459,0.927)	0.698	(0.387,0.922)	0.729	(0.189,0.924)	0.549	(0.078,0.923)	0.642	(0.077,0.917)
a	0.016	(4.30E-4,0.051)	0.016	(4.78E-4,0.048)	0.009	(2.86E-4,0.030)	0.021	(4.66E-4,0.069)	0.029	(7.71E-4,0.074)	0.018	(9.01E-4,0.035)
σ_{M_p}	0.430	(0.359,0.499)	0.432	(0.364,0.498)	0.435	(0.358,0.500)	0.464	(0.379,0.536)	0.469	(0.349,0.570)	0.477	(0.396,0.552)
s_n	0.476	(0.435.0.521)	0.470	(0.429,0.514)	0.463	(0.426,0.507)	0.489	(0.437,0.594)	0.520	(0.429,0.907)	0.468	(0.426,0.542)
s_p	0.447	(0.420,0.471)	0.450	(0.424,0.473)	0.452	(0.428,0.477)	0.437	(0.405,0.471)	0.404	(0.063,0.477)	0.450	(0.421,0.479)

Table 8: Percentage daily S&P500 index returns between 3 Jan 2005 and 10 May 2018. Estimation of the dynamic jump model defined by (32)-(36), (38)-(40) and (42)-(47), with jump measurement errors included. The jump measures are constructed using the CPR framework under the significance levels of 1%, 0.5% and 0.1% for the truncation level $c = 3$. The model is also estimated using the CPR method with truncation levels $c = 4$ and $c = 5$, and a significance level of 1%. We report the marginal posterior mean (MPM) and 95% highest posterior density (95% HPD) credible interval for each of the model parameters.

	CPR (c=3)						CPR (c=4)		CPR (c=5)	
	1% significance		0.5% significance		0.1% significance		1% significance		1% significance	
	MPM	95% HPD Interval	MPM	95% HPD Interval	MPM	95% HPD Interval	MPM	95% HPD Interval	MPM	95% HPD Interval
μ	0.062	(0.024,0.105)	0.061	(0.024,0.102)	0.064	(0.028,0.104)	0.062	(0.024,0.103)	0.062	(0.026,0.103)
γ	-0.078	(-0.140,-0.019)	-0.069	(-0.133,-0.015)	-0.064	(-0.122,-0.012)	-0.090	(-0.128,-0.018)	-0.071	(-0.128,-0.016)
ρ	-0.337	(-0.433-0.237)	-0.349	(-0.449,-0.245)	-0.357	(-0.456,-0.253)	-0.348	(-0.445,-0.245)	-0.350	(-0.448,-0.240)
κ	0.059	(0.040,0.081)	0.050	(0.027,0.074)	0.053	(0.032,0.074)	0.047	(0.025,0.074)	0.049	(0.026,0.075)
θ	0.445	(0.371,0.525)	0.459	(0.352,0.608)	0.454	(0.368,0.551)	0.459	(0.326,0.572)	0.465	(0.373,0.585)
σ_v	0.117	(0.106,0.131)	0.118	(0.105,0.134)	0.118	(0.106,0.132)	0.117	(0.103,0.132)	0.117	(0.105,0.130)
μ_p	-2.193	(-2.238,-2.150)	-2.176	(-2.231,-2.121)	-2.176	(-2.224,-2.129)	-2.215	(-2.266,-2.159)	-2.229	(-2.277,-2.169)
γ_p	0.484	(0.426,0.551)	0.447	(0.343,0.541)	0.446	(0.373,0.527)	0.454	(0.342,0.541)	0.470	(0.340,0.556)
σ_p	0.449	(0.370,0.516)	0.454	(0.378,0.521)	0.447	(0.373,0.515)	0.440	(0.366,0.504)	0.435	(0.366,0.504)
π_p	0.312	(0.169,0.464)	0.322	(0.165,0.507)	0.390	(0.179,0.638)	0.319	(0.159,0.508)	0.312	(0.151,0.501)
δ_0^p	0.157	(0.109,0.222)	0.117	(0.067,0.172)	0.059	(0.010,0.104)	0.125	(0.071,0.190)	0.116	(0.065,0.173)
α_p	0.183	(0.056,0.247)	0.147	(0.035,0.249)	0.259	(0.258,0.260)	0.178	(0.045,0.241)	0.141	(0.020,0.223)
β_p	0.026	(0.004,0.052)	0.020	(0.003,0.045)	0.024	(0.003,0.055)	0.020	(0.002,0.042)	0.016	(0.001,0.038)
μ_v	1.285	(0.842,2.205)	1.821	(0.860,6.061)	1.589	(0.956,3.211)	1.670	(0.899,2.820)	1.774	(0.898,3.861)
δ_0^v	0.027	(0.012,0.046)	0.021	(0.006,0.039)	0.022	(0.009,0.041)	0.019	(0.008,0.042)	0.020	(0.007,0.041)
α_v	0.053	(0.014,0.274)	0.178	(0.017,0.665)	0.105	(0.014,0.616)	0.167	(0.015,0.696)	0.129	(0.0149,0.551)
β_v	0.023	(0.008,0.048)	0.027	(0.004,0.086)	0.023	(0.006,0.056)	0.024	(0.003,0.067)	0.023	(0.004,0.061)
β_{vp}	0.001	(2.48E-5,0.004)	0.002	(3.10E-5,0.011)	0.003	(5.23E-5,0.016)	0.003	(3.42E-5,0.013)	0.002	(3.10E-5,0.011)
ψ_0	-0.645	(-0.723,-0.560)	-0.695	(-0.843,-0.582)	-0.691	(-0.801,-0.593)	-0.699	(-0.855,-0.578)	-0.674	(-0.837,-0.566)
ψ_1	1.318	(1.232,1.412)	1.273	(1.103,1.386)	1.279	(1.152,1.380)	1.260	(1.094,1.383)	1.283	(1.127,1.390)
σ_{BV}	0.530	(0.500,0.566)	0.542	(0.504,0.598)	0.537	(0.502,0.584)	0.547	(0.504,0.605)	0.540	(0.503,0.591)
b	0.780	(0.554,0.949)	0.756	(0.530,0.928)	0.709	(0.462,0.919)	0.760	(0.498,0.939)	0.745	(0.521,0.930)
a	0.013	(3.05E-4,0.046)	0.015	(4.79E-4,0.052)	0.018	(5.025E-4,0.051)	0.017	(4.99E-4,0.056)	0.016	(4.87E-4,0.052)
σ_{M_p}	0.445	(0.037,0.517)	0.443	(0.367,0.514)	0.450	(0.376,0.519	0.434	(0.361,0.502)	0.439	(0.366,0.502)
s_n	0.485	(0.444,0.528)	0.476	(0.434,0.520)	0.466	(0.430,0.504)	0.476	(0.434,0.523)	0.476	(0.435,0.520)
s_p	0.444	(0.419,0.468)	0.446	(0.421,0.470)	0.450	(0.423,0.476)	0.446	(0.421,0.470)	0.447	(0.422,0.471)

Table 9: Percentage daily IBM stock returns between 3 Jan 2005 and 10 May 2018. Estimation of the dynamic jump model defined by (32)-(36), (38)-(40) and (42)-(47), with jump measurement errors included. The jump measures are constructed using the BNS and MEDRV frameworks, each under the significance levels of 1%, 0.5% and 0.1%. We report the marginal posterior mean (MPM) and 95% highest posterior density (95% HPD) credible interval for each of the model parameters.

	BNS						MEDRV					
	1% significance		0.5% significance		0.1% significance		1% significance		0.5% significance		0.1% significance	
	MPM	95% HPD Interval	MPM	95% HPD Interval	MPM	95% HPD Interval	MPM	95% HPD Interval	MPM	95% HPD Interval	MPM	95% HPD Interval
μ	0.046	(0.004,0.094)	0.056	(0.011,0.106)	0.051	(0.009,0.102)	0.047	(0.005,0.094)	0.046	(0.005,0.095)	0.053	(0.010,0.100)
γ	-0.051	(-0.097,-0.002)	-0.045	(-0.103,-0.003)	-0.039	(-0.093,-0.003)	-0.037	(-0.090,-0.002)	-0.037	(-0.093,-0.002)	-0.040	(-0.094,-0.003)
ρ	-0.084	(-0.200,-0.034)	-0.074	(-0.209,0.057)	-0.109	(-0.239,0.027)	-0.060	(-0.163,0.047)	-0.097	(-0.221,0.025)	-0.088	(-0.219,0.041)
κ	0.638	(0.581,0.680)	0.604	(0.574,0.631)	0.666	(0.630,0.709)	0.639	(0.546,0.722)	0.623	(0.593,0.660)	0.660	(0.624,0.705)
θ	0.614	(0.610,0.619)	0.614	(0.610,0.619)	0.615	(0.610,0.619)	0.614	(0.609,0.618)	0.615	(0.610,0.619)	0.615	(0.610,0.619)
σ_v	0.041	(0.038,0.052)	0.040	(0.038,0.042)	0.040	(0.038,0.042)	0.051	(0.049,0.053)	0.040	(0.038,0.042)	0.040	(0.038,0.042)
μ_p	-1.654	(-1.697,-1.612)	-1.663	(-1.706,-1.623)	-1.670	(-1.716,-1.621)	-1.491	(-1.538,-1.441)	-1.513	(-1.559,-1.467)	-1.506	(-1.561,-1.460)
γ_p	0.291	(0.254,0.326)	0.297	(0.262,0.338)	0.311	(0.255,0.355)	0.251	(0.200,0.301)	0.283	(0.236,0.335)	0.270	(0.225,0.331)
σ_p	0.516	(0.443,0.576)	0.471	(0.385,0.554)	0.476	(0.391,0.552)	0.526	(0.467,0.576)	0.519	(0.450,0.574)	0.486	(0.398,0.555)
π_p	0.366	(0.246,0.497)	0.378	(0.195,0.593)	0.376	(0.166,0.621)	0.427	(0.304,0.555)	0.395	(0.224,0.597)	0.377	(0.188,0.615)
δ_0^p	0.116	(0.076,0.162)	0.082	(0.021,0.144)	0.046	(0.007,0.092)	0.113	(0.063,0.165)	0.087	(0.027,0.144)	0.047	(0.009,0.086)
α_p	0.095	(0.020,0.231)	0.120	(0.021,0.235)	0.113	(0.021,0.214)	0.081	(0.023,0.214)	0.105	(0.021,0.240)	0.115	(0.026,0.217)
β_p	0.013	(0.002,0.030)	0.014	(0.001,0.035)	0.015	(0.001,0.037)	0.017	(0.005,0.036)	0.013	(0.001,0.033)	0.014	(0.001,0.035)
μ_v	1.991	(1.785,2.230)	1.859	(1.637,2.195)	1.912	(1.668,2.261)	2.363	(1.793,3.086)	1.993	(1.645,2.383)	2.191	(1.825,2.533)
δ_0^v	0.126	(0.109,0.144)	0.130	(0.114,0.145)	0.131	(0.117,0.148)	0.116	(0.100,0.131)	0.123	(0.110,0.136)	0.125	(0.111,0.139)
α_v	0.209	(0.194,0.231)	0.213	(0.193,0.223)	0.227	(0.211,0.245)	0.208	(0.190,0.222)	0.248	(0.238,0.258)	0.199	(0.172,0.215)
β_v	0.193	(0.182,0.210)	0.197	(0.176,0.203)	0.208	(0.196,0.220)	0.192	(0.177,0.203)	0.227	(0.218,0.229)	0.183	(0.160,0.192)
β_{vp}	0.003	(9.64E-5,0.010)	0.004	(1.08E-4,0.016)	0.008	(2.18E-4,0.030)	0.003	(8.95E-5,0.009)	0.005	(1.24E-4,0.016)	0.005	(1.17E-4,0.020)
ψ_0	-0.110	(-0.138,-0.082)	-0.119	(-0.156,-0.085)	-0.101	(-0.150,-0.058)	-0.159	(-0.203,-0.115)	-0.139	(-0.187,-0.090)	-0.156	(-0.189,-0.115)
ψ_1	1.176	(1.131,1.224)	1.180	(1.115,1.242)	1.198	(1.114,1.269)	1.105	(1.021,1.190)	1.191	(1.103,1.279)	1.155	(1.096,1.232)
σ_{BV}	0.586	(0.571,0.604)	0.575	(0.561,0.591)	0.583	(0.568,0.598)	0.625	(0.610,0.641)	0.597	(0.582,0.612)	0.600	(0.584,0.616)
b	0.785	(0.561,0.944)	0.738	(0.478,0.930)	0.700	(0.422,0.924)	0.785	(0.558,0.948)	0.694	(0.446,0.908)	0.691	(0.403,0.916)
a	0.013	(4.33E-4,0.044)	0.024	(7.06E-4,0.068)	0.017	(7.89E-4,0.043)	0.019	(4.98E-4,0.057)	0.024	(7.26E-4,0.063)	0.014	(6.68E-4,0.040)
σ_{M_p}	0.424	(0.350,0.502)	0.465	(0.369,0.544)	0.462	(0.375,0.542)	0.398	(0.331,0.465)	0.404	(0.332,0.482)	0.440	(0.355,0.527)
s_n	0.520	(0.483,0.560)	0.508	(0.471,0.548)	0.503	(0.464,0.543)	0.520	(0.484,0.555)	0.511	(0.475,0.551)	0.504	(0.466,0.543)
s_p	0.478	(0.452,0.503)	0.484	(0.457,0.510)	0.488	(0.462,0.513)	0.474	(0.446,0.502)	0.483	(0.454,0.509)	0.488	(0.462,0.514)

Table 10: Percentage daily IBM stock returns between 3 Jan 2005 and 10 May 2018. Estimation of the dynamic jump model defined by (32)-(36), (38)-(40) and (42)-(47), with jump measurement errors included. The jump measures are constructed using the CPR framework under the significance levels of 1%, 0.5% and 0.1% for the truncation level $c = 3$. The model is also estimated using the CPR method with truncation levels $c = 4$ and $c = 5$, and a significance level of 1%. We report the marginal posterior mean (MPM) and 95% highest posterior density (95% HPD) credible interval for each of the model parameters.

	CPR (c=3)						CPR (c=4)		CPR (c=5)	
	1% significance		0.5% significance		0.1% significance		1% significance		1% significance	
	MPM	95% HPD Interval	MPM	95% HPD Interval	MPM	95% HPD Interval	MPM	95% HPD Interval	MPM	95% HPD Interval
μ	0.038	(-0.003,0.086)	0.045	(0.001,0.094)	0.046	(0.004,0.093)	0.044	(0.005,0.089)	0.041	(4.70E-4,0.088)
γ	-0.035	(-0.089,-0.002)	-0.039	(-0.095,-0.003)	-0.036	(-0.090,-0.002)	-0.033	(-0.083,-0.002)	-0.032	(-0.085,-0.002)
ρ	-0.084	(-0.204,0.037)	-0.086	(-0.203,0.037)	-0.084	(-0.210,0.046)	-0.096	(-0.213,0.028)	-0.113	(-0.237,0.011)
κ	0.663	(0.629,0.711)	0.542	(0.497,0.609)	0.579	(0.523,0.635)	0.675	(0.631,0.715)	0.657	(0.601,0.728)
θ	0.615	(0.610,0.619)	0.615	(0.610,0.620)	0.615	(0.611,0.620)	0.615	(0.610,0.619)	0.614	(0.610,0.619)
σ_v	0.040	(0.038,0.042)	0.039	(0.037,0.042)	0.040	(0.037,0.042)	0.040	(0.038,0.042)	0.040	(0.038,0.042)
μ_p	-1.629	(-1.669,-1.592)	-1.652	(-1.697,-1.603)	-1.648	(-1.691,-1.608)	-1.626	(-1.666,-1.585)	-1.647	(-1.688,-1.605)
γ_p	0.263	(0.235,0.291)	0.287	(0.241,0.329)	0.283	(0.251,0.317)	0.278	(0.247,0.308)	0.291	(0.259,0.326)
σ_p	0.539	(0.482,0.588)	0.529	(0.462,0.586)	0.513	(0.421,0.581)	0.483	(0.410,0.553)	0.486	(0.409,0.555)
π_p	0.388	(0.279,0.501)	0.373	(0.217,0.543)	0.371	(0.188,0.565)	0.438	(0.286,0.591)	0.426	(0.267,0.591)
δ_0^p	0.152	(0.109,0.202)	0.137	(0.070,0.221)	0.083	(0.035,0.144)	0.112	(0.038,0.178)	0.101	(0.037,0.160)
α_p	0.105	(0.023,0.247)	0.118	(0.023,0.221)	0.141	(0.016,0.240)	0.091	(0.010,0.228)	0.119	(0.019,0.243)
β_p	0.012	(0.002,0.028)	0.011	(0.001,0.027)	0.015	(0.002,0.0412)	0.010	(0.001,0.028)	0.015	(0.002,0.035)
μ_v	2.272	(1.983,2.623)	1.778	(1.515,2.264)	1.837	(1.593,2.122)	2.128	(1.928,2.373)	2.100	(1.909,2.323)
δ_0^v	0.121	(0.106,0.136)	0.121	(0.106,0.138)	0.126	(0.109,0.142)	0.133	(0.113,0.148)	0.130	(0.113,0.146)
α_v	0.223	(0.209,0.237)	0.200	(0.181,0.222)	0.233	(0.221,0.242)	0.228	(0.217,0.239)	0.192	(0.180,0.204)
β_v	0.205	(0.194,0.216)	0.186	(0.169,0.202)	0.216	(0.206,0.221)	0.211	(0.206,0.216)	0.177	(0.168,0.189)
β_{vp}	0.002	(6.01E-5,0.008)	0.002	(5.44E-5,0.008)	0.003	(8.33E-5,0.012)	0.004	(8.83E-5,0.012)	0.004	(9.02E-5,0.012)
ψ_0	-0.140	(-0.171,-0.111)	-0.136	(-0.166,-0.106)	-0.141	(-0.175,-0.104)	-0.137	(-0.164,-0.111)	-0.128	(-0.161,-0.092)
ψ_1	1.135	(1.090,1.184)	1.179	(1.108,1.230)	1.161	(1.105,1.217)	1.136	(1.095,1.178)	1.150	(1.101,1.202)
σ_{BV}	0.586	(0.572,0.601)	0.575	(0.560,0.591)	0.582	(0.567,0.597)	0.581	(0.566,0.597)	0.580	(0.564,0.596)
b	0.813	(0.623,0.951)	0.713	(0.457,0.922)	0.690	(0.405,0.916)	0.761	(0.530,0.945)	0.775	(0.555,0.943)
a	0.015	(2.62E-4,0.049)	0.019	(4.39E-4,0.063)	0.015	(3.37E-4,0.044)	0.029	(9.41E-4,0.084)	0.029	(9.90E-4,0.078)
σ_{M_p}	0.403	(0.332,0.472)	0.410	(0.339,0.487)	0.429	(0.347,0.523)	0.453	(0.372,0.530)	0.463	(0.386,0.536)
s_n	0.528	(0.493,0.565)	0.519	(0.482,0.560)	0.510	(0.473,0.550)	0.516	(0.482,0.552)	0.514	(0.478,0.550)
s_p	0.472	(0.442,0.498)	0.479	(0.450,0.505)	0.485	(0.457,0.510)	0.476	(0.446,0.505)	0.478	(0.449,0.507)